# Chapter 2
# The Displacement of Atoms

## 2.1 Elementary Displacement Theory

The struck lattice atom of energy $T$ is referred to as a primary knock-on atom, or PKA. This atom moves through the lattice encountering other lattice atoms. Such encounters may result in sufficient energy transfer to displace this lattice atom from its site resulting in two displaced atoms. If this collision sequence continues, a series of tertiary knock-ons is produced resulting in a collision cascade. A cascade is a spatial cluster of lattice vacancies and atoms residing as interstitials in a localized region of the lattice. Such a phenomenon can have a profound effect on the physical and mechanical properties of the alloy, as will become evident later. Here, we are concerned with being able to quantify the displacement cascade. That is, for a neutron of energy $E_i$, striking a lattice atom, how many lattice atom displacements will result? We have already discussed in detail the nature of neutron–nucleus and atom–atom collisions. Now, we will develop a model for determining the number of atoms displaced by a PKA of energy $T$.

Recall that to quantify radiation damage, we require a solution to the damage rate equation:

$$R_d = N \int_{\stackrel{\vee}{E}}^{\hat{E}} \phi(E_i)\sigma_D(E_i)\,dE_i, \qquad (2.1)$$

where $N$ is the lattice atom number density, $\phi(E_i)$ is the energy-dependent particle flux, and $\sigma_D(E_i)$ is the energy-dependent displacement cross section. The displacement cross section is a probability for the displacement of lattice atoms by incident particles:

$$\sigma_D(E_i) = \int_{\stackrel{\vee}{T}}^{\hat{T}} \sigma(E_i, T)\, v\,(T)\,dT, \qquad (2.2)$$

where $\sigma(E_i, T)$ is the probability that a particle of energy $E_i$ will impart a recoil energy $T$ to a struck lattice atom, and $v(T)$ is the number of displaced atoms resulting from such a collision. Chapter 1 provided the energy transfer cross section appearing in Eq. (2.2) for various types of particles in various energy ranges. This chapter will be devoted to supplying the second term in the integrand, $v(T)$, the number of atom displacements resulting from a primary recoil atom of energy $T$, and the limits of $T$ between which displacements occur. Finally, we will develop the displacement cross section and an expression for the displacement rate.
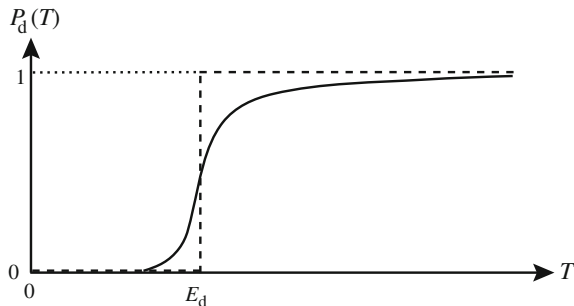
### 2.1.1   Displacement Probability

As a first step, we define $P_d(T)$ as the probability that a struck atom is displaced upon receipt of energy $T$. Clearly, there is some minimum energy that must be transferred in order to produce a displacement. We will call this energy, $E_d$. The magnitude of $E_d$ is dependent upon the crystallographic structure of the lattice, the direction of the incident PKA, the thermal energy of the lattice atom, etc. These considerations will be discussed in detail later. By definition of $E_d$, the probability of displacement for $T < E_d$ is zero. If $E_d$ is a fixed value under all conditions, then the probability of displacement for $T \geq E_d$ is one. Hence, our simplest model for the displacement probability is a step function:

$$\begin{aligned}
P_d(T) &= 0 \quad \text{for} \quad T < E_d \\
&= 1 \quad \text{for} \quad T \geq E_d,
\end{aligned} \tag{2.3}$$

and is shown in Fig. 2.1. However, $E_d$ is not constant for all collisions due to the factors mentioned earlier. The effect of atomic vibrations of the lattice atoms would be expected to lower the value of $E_d$ or introduce a natural "width" of the order $kT$ to the displacement probability. Further, as will be discussed later, the effect of crystallinity will also contribute strongly to the blurring effect on $E_d$. In fact, the picture in Fig. 2.1 and Eq. (2.3) is only strictly true for an amorphous solid at 0 K. A more realistic representation is shown in Fig. 2.2 and is represented as:
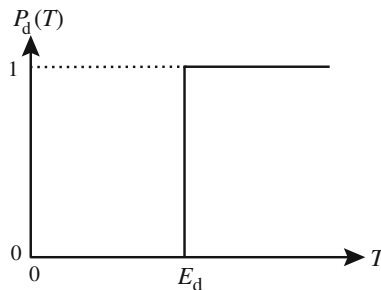


**Fig. 2.1** The displacement probability $P_d(T)$ as a function of the kinetic energy transferred to a lattice atom, assuming a sharp displacement threshold

**Fig. 2.2** The displacement probability as a function of the kinetic energy transferred to the lattice atom allowing for a blurring of the threshold due to atomic vibrations, impurity atoms, etc.

$$
\begin{aligned}
P_\mathrm{d}(T) &= 0 \quad && \text{for} \quad T < E_{\mathrm{d_{min}}} \\
&= f(T) \quad && \text{for} \quad E_{\mathrm{d_{min}}} \le T < E_{\mathrm{d_{max}}} \\
&= 1 \quad && \text{for} \quad T \ge E_{\mathrm{d_{max}}},
\end{aligned}
\tag{2.4}
$$

where $f(T)$ is a smoothly varying function between 0 and 1. Given the displacement probability, the next task is to find the number of displacements as a function of the energy transferred. Kinchin and Pease [1] developed a simple theory to find the average number of displaced atoms initially created by a PKA of energy $T$ in a given solid lattice. Their analysis is based on the following assumptions:

1. The cascade is created by a sequence of two-body elastic collisions between atoms.
2. The displacement probability is 1 for $T \ge E_\mathrm{d}$ as given by Eq. (2.3).
3. When an atom with initial energy $T$ emerges from a collision with energy $T'$ and generates a new recoil with energy $\varepsilon$, it is assumed that no energy passes to the lattice and $T = T' + \varepsilon$.
4. Energy loss by electron stopping is given by a cutoff energy $E_\mathrm{c}$. If the PKA energy is greater than $E_\mathrm{c}$, no additional displacements occur until electron energy losses reduce the PKA energy to $E_\mathrm{c}$. For all energies less than $E_\mathrm{c}$, electronic stopping is ignored, and only atomic collisions occur.
5. The energy transfer cross section is given by the hard sphere model.
6. The arrangement of the atoms in the solid is random; effects due to crystal structure are neglected.

Assumption 1 is fundamental to all theories of a cascade consisting of isolated point defects. Elimination of this restriction allows the cascade to be represented by a displacement spike discussed in Chap. 3. Assumption 2 neglects crystallinity and atomic vibrations, which will add a natural width or "blurring" effect to the distribution. Later on, we will relax Assumptions 3, 4, 5 and 6.

## 2.1.2  The Kinchin and Pease Model for Atom Displacements

Consider the two moving atoms created when a PKA first strikes a stationary atom. After the collision, the PKA has residual energy $T - \varepsilon$ and the struck atom receives an energy $\varepsilon - E_d$, giving:

$$v(T) = v(T - \varepsilon) + v(\varepsilon - E_d), \tag{2.5}$$

where $E_d$ is the energy consumed in the reaction. By neglecting $E_d$ relative to $\varepsilon$, i.e., $\varepsilon \gg E_d$ according to Assumption 3, then Eq. (2.5) becomes:

$$v(T) = v(T - \varepsilon) + v(\varepsilon). \tag{2.6}$$

Equation (2.6) is not sufficient to determine $v(T)$ because the energy transfer $\varepsilon$ is unknown. Since the PKA and lattice atoms are identical, $\varepsilon$ may lie anywhere between 0 and $T$. However, if we know the probability of transferring energy in the range ($\varepsilon$, d$\varepsilon$) in a collision, we can multiply Eq. (2.6) by this probability and integrate over all allowable values of $\varepsilon$. This will yield the average number of displacements.

Using the hard sphere Assumption 5, the energy transfer cross section is as follows:

$$\sigma(T, \varepsilon) = \frac{\sigma(T)}{\gamma T} = \frac{\sigma(T)}{T} \quad \text{for like atoms,} \tag{2.7}$$

and the probability that a PKA of energy $T$ transfers energy in the range ($\varepsilon$, d$\varepsilon$) to the struck atom is as follows:

$$\frac{\sigma(T, \varepsilon)\mathrm{d}\varepsilon}{\sigma(T)} = \frac{\mathrm{d}\varepsilon}{T}, \tag{2.8}$$

for $\gamma = 1$ (like atoms). Multiplying the right-hand side of Eq. (2.6) by d$\varepsilon/T$ and integrating from 0 to $T$ yields:

$$\begin{aligned} v(T) &= \frac{1}{T} \int_0^T [v(T - \varepsilon) + v(\varepsilon)]\mathrm{d}\varepsilon \\ &= \frac{1}{T} \left[ \int_0^T v(T - \varepsilon)\mathrm{d}\varepsilon + \int_0^T v(\varepsilon)\mathrm{d}\varepsilon \right]. \end{aligned} \tag{2.9}$$

A change in variables from $\varepsilon$ to $\varepsilon' = T - \varepsilon$ in the first integral in Eq. (2.9) gives:

$$v(T) = \frac{1}{T} \int_0^T v(\varepsilon')\,\mathrm{d}\varepsilon' + \frac{1}{T} \int_0^T v(\varepsilon)\,\mathrm{d}\varepsilon, \tag{2.10}$$

which is really a sum of two identical integrals. Therefore,

$$v(T) = \frac{2}{T} \int_0^T v(\varepsilon)\, d\varepsilon. \tag{2.11}$$

Before solving Eq. (2.11), let us examine the behavior of $v(\varepsilon)$ near the displacement threshold, $E_d$. Clearly when $T < E_d$, there are no displacements and:

$$v(T) = 0 \quad \text{for} \quad 0 < T < E_d. \tag{2.12}$$

If $T$ is greater than or equal to $E_d$ but less than $2E_d$, two results are possible. The first is that the struck atom is displaced from its lattice site, and the PKA, now left with energy less than $E_d$, falls into its place. However, if the original PKA does not transfer $E_d$, the struck atom remains in place and no displacement occurs. In either case, only one displacement in total is possible from a PKA with energy between $E_d$ and $2E_d$, and:

$$v(T) = 1 \quad \text{for } E_d \leq T < 2E_d. \tag{2.13}$$

Using Eqs. (2.12) and (2.13), we may split the integral in Eq. (2.11) into ranges from 0 to $E_d$, $E_d$ to $2E_d$, and $2E_d$ to $T$ and evaluate:

$$v(T) = \frac{2}{T} \left[ \int_0^{E_d} 0\, d\varepsilon + \int_{E_d}^{2E_d} 1\, d\varepsilon + \int_{2E_d}^T v(\varepsilon)\, d\varepsilon \right],$$

yielding:

$$v(T) = \frac{2E_d}{T} + \frac{2}{T} \int_{2E_d}^T v(\varepsilon)\, d\varepsilon. \tag{2.14}$$

We can solve Eq. (2.14) by multiplying by $T$ and differentiating with respect to $T$ giving:

$$T\frac{dv}{dT} = v, \tag{2.15}$$
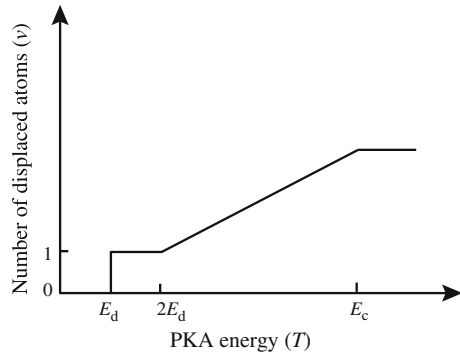
with the solution:

$$v = CT. \tag{2.16}$$

Substituting Eq. (2.16) into Eq. (2.14) gives:

$$C = \frac{1}{E_d}, \tag{2.17}$$

**Fig. 2.3** The number of displaced atoms in the cascade as a function of the PKA energy according to the model of Kinchin and Pease



and therefore:

$$v(T) = \frac{T}{2E_d} \quad \text{for } 2E_d \le T < E_c. \tag{2.18}$$

The upper limit is set by $E_c$ (Assumption 4). When a PKA is born with $T \ge E_c$, the number of displacements is $v(T) = E_c/2E_d$. So the full Kinchin–Pease (K–P) result is as follows:

$$v(T) = \begin{cases} 0 & \text{for } T < E_d \\ 1 & \text{for } E_d \le T < 2E_d \\ \dfrac{T}{2E_d} & \text{for } 2E_d \le T < E_c. \\ \dfrac{E_c}{2E_d} & \text{for } T \ge E_c \end{cases} \tag{2.19}$$

Note that if $E_c$ is ignored, $T/2E_d$ is a true average since the number of displacements can range from 0 (no energy transfers above $E_d$) to $T/E_d - 1$ (every collision transfers just enough), and for large $T$, $T/E_d \gg 1$. So the maximum value of $v(T)$ is $T/E_d$. The full displacement function described by Eq. (2.19) is shown in Fig. 2.3.

## 2.1.3  The Displacement Energy

A lattice atom must receive a minimum amount of energy in the collision in order to be displaced from its lattice site. This is the displacement energy or displacement threshold, $E_d$. If the energy transferred, $T$, is less than $E_d$, the struck atom will vibrate about its equilibrium position but will not be displaced. These vibrations will be transmitted to neighboring atoms through the interaction of their potential fields, and the energy will appear as heat. Hence, the potential fields of the atoms in the lattice form a barrier over which the stuck atom must pass in order to be displaced. This is the source of the displacement threshold energy.

Since metals are crystalline, the potential barrier surrounding an equilibrium lattice site is not uniform in all directions. In fact, there are directions in which the surrounding atoms will remove large amounts of energy from the struck atom yielding a high potential barrier. Along directions of high symmetry, there exist open directions along which the threshold displacement energy is low. Since the direction of the recoil is determined from the collision event which is itself a random process, the recoil direction is entirely random. The single value often quoted for displacement energy in radiation damage calculations then represents a spherical average of the potential barrier surrounding the equilibrium lattice site.

The value of $E_d$ may be roughly estimated using an argument by Seitz [2]. The energy of sublimation, $E_s$, for most metals is about 5–6 eV. Since half as many bonds are broken by removing an atom from the surface of a crystal as opposed to the interior, the energy to remove an atom from the interior is then 10–12 eV. If an atom is moved from its lattice site to an interstitial position in the direction of least resistance and time is allowed for neighboring atoms to relax (an adiabatic movement), an energy of $2E_s$ is needed. Since in reality, the struck atom is not always projected in the direction of least resistance and time is not allowed for the relaxation of neighboring atoms, a greater amount of energy (perhaps 4–5 $E_s$) is needed. Thus, we would expect $E_d$ to be 20–25 eV.

Accurate determination of the displacement energy can be made if the interaction potential between lattice atoms is known. This is accomplished by moving the atom in a given direction and summing the interaction energies between the moving atom and all other nearest neighbors along the trajectory of the struck atom. When the total potential energy reaches a maximum, the position corresponds to a saddle point and the difference between the energy of the atom at the saddle point, $E^*$, and its energy in the equilibrium position, $E_{eq}$, represents the displacement threshold for the particular direction. Since the interaction energy in these collisions is only tens of eV, the Born–Mayer potential would be the most appropriate potential to use in describing the interaction. These calculations can be carried out over all directions and averaged to obtain a mean $E_d$ for a particular solid.

To appreciate the significance of the variation in interaction energies or potential barriers with crystal direction, we will consider the case of copper. In the cubic lattice, there are three crystallographic directions that may be considered easy directions for displacement: $\langle 100 \rangle$, $\langle 110 \rangle$ and $\langle 111 \rangle$. In particular, $\langle 110 \rangle$ is the close-packed direction in the fcc lattice and $\langle 111 \rangle$ is the close-packed direction in the bcc lattice. Figure 2.4 shows how an atom is displaced along each of these directions in the fcc lattice. In each case, the displaced atom K passes through the midpoint of a set of "barrier atoms," B, in the direction of the L atom, with the atom configuration dependent on the direction. For a K atom displaced in the $\langle 110 \rangle$ direction, the atoms are located at the corners of a rectangle to which the path of K is perpendicular. When the K atom passes through the barrier, it loses kinetic energy in glancing collisions, which initially becomes potential energy of the barrier atoms. The energy need not be shared equally between the four B atoms. This is illustrated by drawing a set of contours of constant $E_d$ in the place of the B atoms (Fig. 2.5). Then, if K only receives a quantity of energy $E_d \langle 110 \rangle$ in the
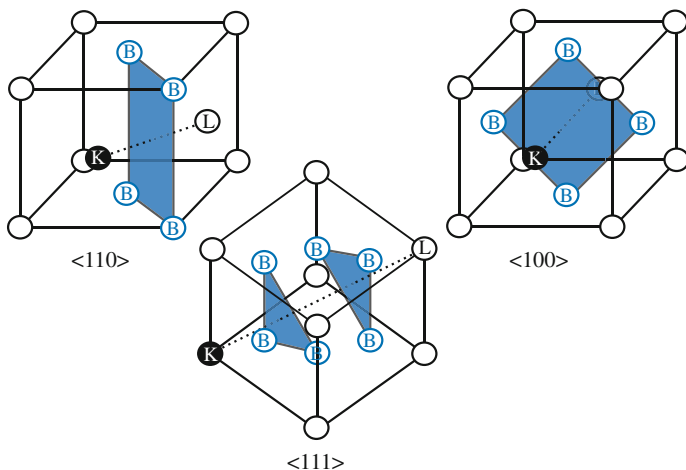
**Fig. 2.4** Struck atom, K, and barrier atoms, B, for various directions of the struck atom in the fcc lattice



**Fig. 2.5** Equi-potential contours in the barrier plane for a struck atom, K, traveling close to the <110> direction and heading toward the barrier plane defined by the barrier atoms, B (after [3])
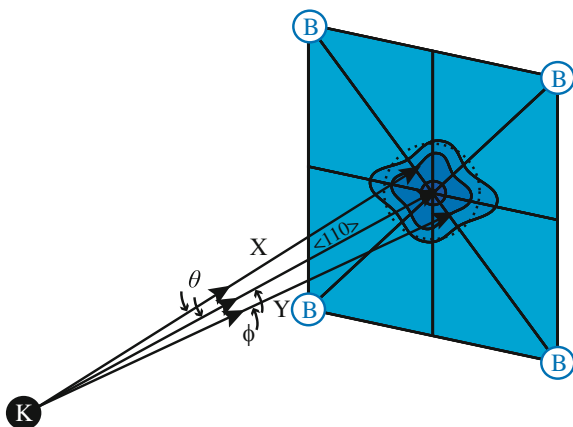
collision event, it will be displaced if its initial direction is contained within a small cone of solid angle centered about the $\langle 110 \rangle$ direction. For small energies, the cone intersects the B atom plane in a circle, but as the energy transferred increases, the intersection deviates significantly from a right circular cone (Fig. 2.5). The contours are in fact generated by the intersection of a complex but symmetrical three-dimensional surface with a sphere which is described about the atom K as center. This contour pattern can be constructed by accounting for the interaction between the K atom and each of the B atoms at every point in time while simultaneously accounting for interactions between each of these five atoms and other atoms in the surrounding region of the crystal. This is a very difficult problem, the solution of which depends heavily on the interaction potential. In principle, at least,
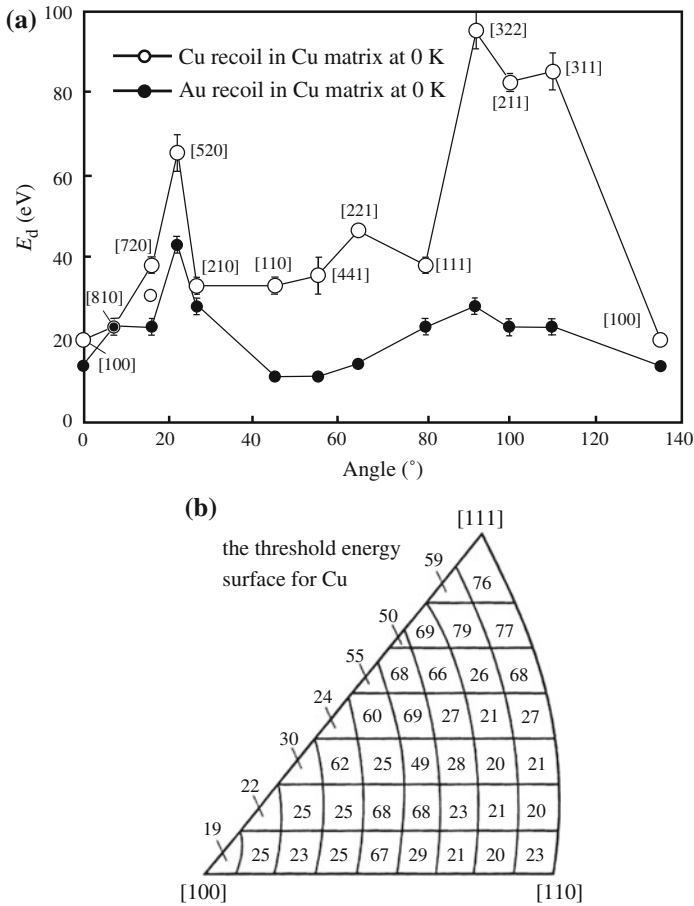
**Fig. 2.6** Displacement energy as a function of direction in (**a**) fcc Cu and Au crystal (after [3]) and (**b**) in copper (after [4])

we can obtain all the information we need about the directional dependence of the thresholds. Figure 2.6 shows the displacement threshold as a function of direction in fcc copper and gold. Note that displacement threshold energies along $\langle 100 \rangle$ and $\langle 110 \rangle$ are low, but the value along $\langle 111 \rangle$ is high due to the large distance between barrier atoms in this direction and the two sets of barriers between the atoms on the body diagonal of the unit cell.

This dependence will be further illustrated in an example using the fcc lattice and a parabolic repulsion function. Figure 2.7 shows a lattice atom on the face of a unit cell in an fcc crystal receiving energy from a collision. Its flight trajectory is in the $\langle 110 \rangle$ direction, which is equidistant from four atoms located on the faces of the unit cell. In an fcc lattice, each atom is surrounded by 12 nearest neighbors. Displacement will be dependent on several important factors. They are the number
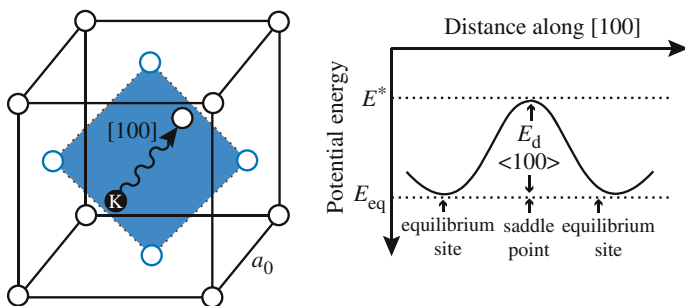
**Fig. 2.7** Displacement of a lattice atom along the <100> direction in the fcc lattice and the variation of energy of the atom with position along its path (after [5])

**Table 2.1** Parameters used for the determination of $E_d$ in the fcc lattice

| Direction | # B atoms | Impact parameter, z | Distance to barrier, y |
|---|---|---|---|
| $\langle 100 \rangle$ | 4 | $\dfrac{a}{2}$ | $\dfrac{a}{2}$ |
| $\langle 110 \rangle$ | 4 | $\dfrac{\sqrt{6}}{4}a$ | $\dfrac{\sqrt{2}}{4}a$ |
| $\langle 111 \rangle$ | 3 | $\dfrac{a}{\sqrt{6}}$ | $\dfrac{a}{3}$ |

of barrier atoms, B, the impact parameter, $z$ (the distance of closest approach to the B atoms), and the distance from the K atom in its lattice site to the barrier, $y$. These quantities are given in Table 2.1 for the fcc lattice. The energy required to displace an atom will increase with $B$ and $y$ and decrease with $z$. Since $z$ is smallest for the $\langle 110 \rangle$ direction, this will be the most difficult to penetrate. Also $z_{100} < z_{110}$ and $y_{100} > y_{110}$, so both factors will make displacement along $\langle 110 \rangle$ easier than along $\langle 100 \rangle$. Let us take the specific example of displacement in the $\langle 100 \rangle$ direction of the fcc example and calculate a value for $E_d$.

The energy of a single atom in a normal lattice site is as follows:

$$E_{eq} = -12U, \tag{2.20}$$

where $U$ is the energy per atom of the crystal. Since only half as many bonds are broken in the sublimation process, this energy is just:

$$E_s \cong 6U, \tag{2.21}$$

and since $E_s \sim 4$–$5$ eV, $U$ is about 1 eV.

To describe the interaction of the lattice atoms as they are pushed together in the solid, we will use a simple parabolic repulsion as opposed to the Born–Mayer potential:

$$V(r) = -U + \frac{1}{2}k(r_{eq} - r)^2 \quad r < r_{eq}$$

$$V(r) = 0 \quad r \geq r_{eq}, \tag{2.22}$$

where $k$ is the force constant characterizing the repulsive position of the potential. The force constant can be expressed as [5]:

$$ka^2 = \frac{3v}{\beta}, \tag{2.23}$$

where
$k$    force constant
$a$    lattice constant
$v$    $a^3/4$ = specific volume of an atom
$\beta$    compressibility

In our example, the equilibrium spacing of the struck atom and the four atoms forming the square barrier is $r_{eq} = a/\sqrt{2}$. When the atom is at the center of the square, it interacts with the four atoms at the corners a distance $a/2$ away. Hence, the energy at the saddle point is as follows:

$$E^* = 4V\left(\frac{a}{2}\right) = 4\left[-U + \frac{1}{2}(ka^2)\left(\frac{1}{\sqrt{2}} - \frac{1}{2}\right)^2\right]. \tag{2.24}$$

The displacement energy in the $\langle 100 \rangle$ direction is then:

$$E_d\langle 100 \rangle = \varepsilon^* - \varepsilon_{eq} = 8U + 2(ka^2)\left(\frac{1}{\sqrt{2}} - \frac{1}{2}\right)^2. \tag{2.25}$$

Typical values for $ka^2$ and $U$ for metals are 60 and 1 eV, respectively, yielding $E_d$ $\langle 100 \rangle \cong 13.1$ eV. This value is in reasonable agreement with that given in Fig. 2.6. Table 2.2 gives values of $E_d$ for various metals [6]. Note that for the transition metals, the accepted value of $E_d$ is 40 eV.

## 2.1.4 The Electron Energy Loss Limit

Now that we have established a lower limit on the energy transfer necessary to cause a displacement, $E_d$, let us turn our attention to the high-energy regime of collisions. Recall that at low energies ($T < 10^3$eV), $S_n \gg S_e$, and we may assume that nearly all of the energy loss of the PKA goes toward elastic collisions (Fig. 1.18). However, as the PKA energy increases, the fraction of the total energy loss that is due to electron excitation and ionization increases until above the crossover energy, $E_x$, $S_e > S_n$.

**Table 2.2** Recommended values of the effective displacement energy for use in displacement calculations (from [6])

| Metal | Lattice ($c/a$) | $E_d$, min (eV) | $E_d$ (eV) |
|---|---|---|---|
| Al | fcc | 16 | 25 |
| Ti | hcp (1.59) | 19 | 30 |
| V | bcc | – | 40 |
| Cr | bcc | 28 | 40 |
| Mn | bcc | – | 40 |
| Fe | bcc | 20 | 40 |
| Co | fcc | 22 | 40 |
| Ni | fcc | 23 | 40 |
| Cu | fcc | 19 | 30 |
| Zr | hcp | 21 | 40 |
| Nb | bcc | 36 | 60 |
| Mo | bcc | 33 | 60 |
| Ta | bcc | 34 | 90 |
| W | bcc | 40 | 90 |
| Pb | fcc | 14 | 25 |
| Stainless steel | fcc | – | 40 |

Our expression for $v(T)$ in Eq. (2.19) must therefore be modified to account for this variation in the amount of kinetic energy available for displacement collisions.

Figure 2.8 shows $(dE/dx)_n$ for carbon recoils in graphite using Eq. (1.163) and Lindhard's Thomas–Fermi result, the latter showing that Eq. (1.163), which predicts a constant value of 250 eV/nm, is a good approximation for energies up to at least $E_a$. Note that at high energies ($T \gg E_x$), electronic energy losses predominate by several orders of magnitude. However, at low energies ($T \ll E_x$), the situation is reversed.

Fortunately, because of departures from the hard sphere model, the primary recoil creates secondaries with average energies far below $\hat{T}/2$. These will almost

**Fig. 2.8** Energy loss from electronic and nuclear stopping as a function of energy (after [7])
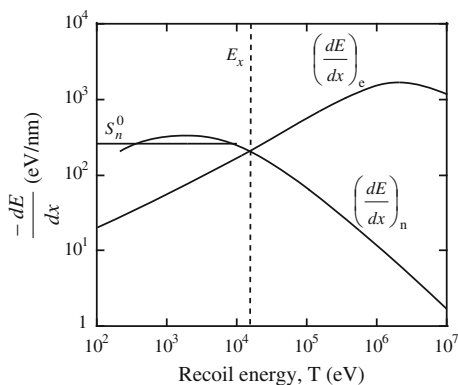
always be in the range where electronic excitation can be neglected. To obtain $v(T)$ to a fair approximation, we calculate the energy $E_c$, dissipated in elastic collisions by the PKA:

$$E_c = \int_0^{\check{T}} \frac{(dE/dx)_n dE}{(dE/dx)_n + (dE/dx)_e}.$$ (2.26)

We can then use Eq. (1.190) for $(dE/dx)_e$ and Eq. (1.130) for $(dE/dx)_n$ with $\check{T} = E_a$. The modified damage function is the original Eq. (2.19) with $T$ replaced by $E_c$:

$$v(T) = \frac{E_c}{2E_d}.$$ (2.27)

As an estimate of $E_c$, we can use the maximum energy a moving atom (of energy $E$) can transfer to an electron as

$$\frac{4m_e}{M}E,$$ (2.28)

and equating this with the ionization energy of the struck electron belonging to the target atom, we have:

$$E_c = \frac{M}{4m_e}I.$$ (2.29)

Kinchin and Pease [1] equated $E_c$ and $E_x$, implying that all energy above $E_x$ is lost in electron excitation, and displacements account for all the energy loss below $E_c$. Figure 2.9 shows $v(T)$ for graphite using Lindhard's $(dE/dx)_n$. Note that for recoils with energy below $E_c$, the simple theory gives a fair description, but for $T > E_c$, the losses in electron excitation are important.



Fig. 2.9 Number of displaced atoms per primary recoil compared to the simple K–P result of $T/2E_d$ (after [7])
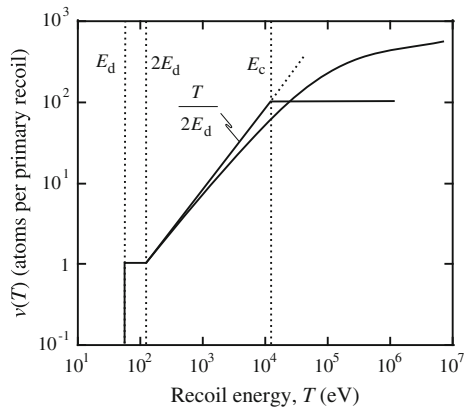
## 2.2 Modifications to the K–P Displacement Model

### 2.2.1 Consideration of $E_d$ in the Energy Balance

Snyder and Neufeld [8] make the assumption that an energy $E_d$ is consumed in each collision such that the relation in Assumption 3 of the K–P displacement model will read:

$$T = T' + \varepsilon + E_d, \tag{2.30}$$

and both atoms move off after collision, no matter how small their energy. When compared with the Kinchin–Pease model, it may be expected that $v(T)$ would decrease since an energy loss term is added. However, because atoms are allowed to leave the collision with energy less than $E_d$, an increase in $v(T)$ will occur. Since these two changes to $v(T)$ nearly cancel, the result is very similar to the K–P model:

$$v(T) = 0.56 \left( 1 + \frac{T}{E_d} \right) \quad \text{for } T > 4E_d. \tag{2.31}$$

### 2.2.2 Realistic Energy Transfer Cross Sections

The weakest point of the K–P displacement model is the assumption of hard sphere collisions (Assumption 5). In fact, more realistic energy transfer cross sections can be used while still maintaining the proportionality of Eq. (2.19). Sanders [9] solved Eq. (2.5) using an inverse power potential ($r^{-s}$) to obtain:

$$v(T) = s \left( 2^{\frac{1}{s+1}} - 1 \right) \frac{T}{2E_d}, \tag{2.32}$$

which for the inverse square potential becomes:

$$v(T) = 0.52 \frac{T}{2E_d}, \tag{2.33}$$

reducing the Kinchin–Pease result by a factor of 2.

However, the use of this potential has its shortcomings because it is applied to all collisions in the cascade, while its region of validity is limited to those values of $T$ such that $\rho < 5a$. Physically, the effect of realistic scattering is to make a larger number collisions generate $T$ in the subthreshold regions below $E_d$ where they are removed from multiplication chain.

For many years, investigators have been intrigued that Eq. (2.19) appears to overestimate $v(T)$ in metals by a factor of 2–10 [10] and yet attempts to measure the energy dependence of $v(T)$ over a large energy range (50–200 keV recoil atoms in gold) gave a quadratic rather than linear relationship. In 1969, Sigmund [11] took a

different approach to this problem by considering the *recoil density F(T, ε) dε* defined as the average number of atoms recoiling with an energy in ($\varepsilon$, $\varepsilon + d\varepsilon$) as a consequence of a primary ion slowing down from $T$ to zero energy. The recoil density can be expressed in a form that uses the power law approximation of the Thomas–Fermi differential cross section [12]:

$$\sigma(T, \varepsilon) \propto T^{-m} \varepsilon^{-1-m}, \tag{2.34}$$

where $0 \leq m \leq 1$, giving:

$$F(T, \varepsilon) = \frac{m}{\psi(1) - \psi(1-m)} \frac{T}{(\varepsilon + U_b)^{1-m} \varepsilon^{1+m}}, \tag{2.35}$$

for $T \gg \varepsilon \gg U_b$, where

$$\psi(x) = d[\ln \Gamma(x)]/dx, \tag{2.36}$$

$U_b$ is the binding energy lost by an atom when leaving a lattice site, and $\Gamma(x)$ is the gamma function or the generalized factorial function. Since a recoiling atom is displaced when $\varepsilon > E_{\mathrm{d}}$, we obtain

$$v(T) = \int_{E_{\mathrm{d}}}^{T} d\varepsilon F(T, \varepsilon) = \frac{(1 + U_b/E_{\mathrm{d}})^m - 1}{\psi(1) - \psi(1-m)} \left( \frac{T}{U_b} \right), \tag{2.37}$$

for $T \gg E_{\mathrm{d}} \gg U_b$. The value of $m$ is chosen in such a way [13] that $\sigma(T, \varepsilon)$ describes collisions at *low* energies, i.e., $2E_{\mathrm{d}} \leq T \leq 100E_{\mathrm{d}}$. This constrains $m \leq 1/4$. For $m = 0$, Eq. (2.37) reads:

$$v(T) = \frac{6}{\pi^2} \frac{T}{U_b} \ln(1 + U_b/E_{\mathrm{d}}). \tag{2.38}$$

This is an upper limit for displacement processes since loss of defects by replacement collisions has been neglected.

A characteristic feature of displacements in metals is the large recombination volume of an isolated point defect, of the order of 100 atomic volumes or more. Hence, $E_{\mathrm{d}}$ is the energy lost to the environment by an atom trying to escape the recombination volume. This has the consequence that in cascades, many defects are lost by replacement collisions [14]. The binding energy $U_b$ is only a few eV and thus negligible as compared to $E_{\mathrm{d}}$, reducing Eq. (2.38) to:

$$v(T) = \frac{6}{\pi^2} \frac{T}{E_{\mathrm{d}}} = 1.22 \left( \frac{T}{2E_{\mathrm{d}}} \right), \tag{2.39}$$

which is about 22 % greater than the result of Eq. (2.19) which accounted for replacement collisions.

### 2.2.3  Energy Loss by Electronic Excitation

Even for $E > E_c$, collisions of the PKA with electrons compete for energy loss against collisions with lattice atoms. These two processes can be treated independently, and each can be represented by separate energy transfer cross sections. The formulation originally presented by Lindhard et al. [15] is summarized here as presented by Olander in [5] as a more realistic treatment of energy loss by electronic excitation (Assumption 4).

As a PKA traverses a distance $dx$ of a solid, three things may happen: (1) It collides with an electron, (2) it collides with an atom, or (3) nothing. Let $p_e\, d\varepsilon_e$ be the probability that a collision between the PKA and an electron in the interval $dx$ transfers energy in the range $(\varepsilon_e, d\varepsilon_e)$ to the electron:

$$p_e d\varepsilon_e = N\sigma_e(T, \varepsilon_e)d\varepsilon_e dx, \tag{2.40}$$

where $\sigma_e(T, \varepsilon_e)$ is the energy transfer cross section from the PKA to the electron. Similarly, for a PKA and lattice atom:

$$p_a d\varepsilon_a = N\sigma_a(T, \varepsilon_a)d\varepsilon_a dx, \tag{2.41}$$

and the probability that nothing happens in $dx$ is as follows:

$$
\begin{aligned}
p_0 &= 1 - \int_0^{\varepsilon_{e,\max}} p_e d\varepsilon_e - \int_0^{\varepsilon_{a,\max}} p_a d\varepsilon_a \\
&= 1 - N\, dx[\sigma_e(T) - \sigma_a(T)],
\end{aligned}
\tag{2.42}
$$

and $\varepsilon_{e,\max}$ and $\varepsilon_{a,\max}$ are the maximum energies transferable to an electron and atom, respectively, by a PKA of energy $T$. We rewrite the conservation equation for $v(T)$ by weighting with the appropriate probability for the process by which it is created and integrating over the permissible ranges of energy transfers:

$$
\begin{aligned}
v(T) = &\int_0^{\varepsilon_{a,\max}} [v(T - \varepsilon_a) + v(\varepsilon_a)]\, p_a\, d\varepsilon_a \\
&+ \int_0^{\varepsilon_{e,\max}} v(T - \varepsilon_e)p_e\, d\varepsilon_e + p_0 v(T).
\end{aligned}
\tag{2.43}
$$

Substituting for $p_e$, $p_a$, and $p_0$ yields:

$$
\begin{aligned}
[\sigma_a(T) + \sigma_e(T)]v(T) = &\int_0^{\varepsilon_{a,\max}} [v(T - \varepsilon_a) + v(\varepsilon_a)]\sigma_a(T, \varepsilon_a)\, d\varepsilon_a \\
&+ \int_0^{\varepsilon_{e,\max}} v(T - \varepsilon_e)\sigma_e(T, \varepsilon_e)\, d\varepsilon_e.
\end{aligned}
\tag{2.44}
$$

Since the maximum energy transferred to an electron is very small compared to $T$, $v$ $(T - \varepsilon_e)$ can be expanded in a Taylor series and truncated after the second term:

$$v(T - \varepsilon_e) = v(T) - \frac{dv}{dT}\varepsilon_e, \tag{2.45}$$

and the last term in Eq. (2.44) can be written as:

$$\int_0^{\varepsilon_e,\max} v(T - \varepsilon_e)\, \sigma_e(T, \varepsilon_e) d\varepsilon_e = v(T) \int_0^{\varepsilon_e,\max} \sigma_e(T, \varepsilon_e)\, d\varepsilon_e$$
$$- \frac{dv}{dT} \int_0^{\varepsilon_e,\max} \varepsilon_e \sigma_e(T, \varepsilon_e)\, d\varepsilon_e. \tag{2.46}$$

The first integral on the right of Eq. (2.46) is the total cross section for collisions of the PKA with the electron and cancels the corresponding term on the left in Eq. (2.44). The second integral on the right of Eq. (2.46) is the electronic stopping power of the solid divided by the atom density. Combining Eqs. (2.46) and (2.45), we have:

$$v(T) + \left[\frac{(dT/dx)_e}{N\sigma(T)}\right]\frac{dv}{dT} = \int_0^{T_{\max}} [v(T - \varepsilon) + v(\varepsilon)]\left[\frac{\sigma(T, \varepsilon)}{\sigma(T)}\right] d\varepsilon, \tag{2.47}$$

where the subscript "$a$" on $T$ and $\sigma$ has been dropped with the understanding that these quantities refer to atomic collisions. Equation (2.47) can be solved using the hard sphere assumption, but where $\left(\frac{dE}{dx}\right)_e$ is given by Eq. (1.190), i.e., $\left(\frac{dE}{dx}\right)_e = kE^{1/2}$, giving:

$$v(T) = \frac{2E_d}{T} + \frac{2}{T}\int_{2E_d}^T v(\varepsilon)d\varepsilon - \frac{kT^{1/2}}{\sigma N}\frac{dv}{dT}. \tag{2.48}$$

After simplification, the final result is as follows:

$$v(T) = \left[1 - \frac{4k}{\sigma N(2E_d)^{1/2}}\right]\left(\frac{T}{2E_d}\right), \quad \text{for } T \gg E_d, \tag{2.49}$$

where $k$ is a constant depending on the atom number density, $N$, and the atomic number. The term $\sigma$ is the energy-independent hard sphere collision cross section. Note that when electronic stopping is properly accounted for in the basic integral equation, the entire concept of a definite energy, $E_c$, separating regimes of electronic energy loss from atomic collisions can be dismissed.

However, Eq. (2.49) is still plagued by the use of the hard sphere assumption. Lindhard realized that in order to ensure that reliable predictions are obtained, a realistic energy transfer cross section must be used. Lindhard also realized that the

parameter $v(T)$ need not be interpreted solely as the number of displacements produced per PKA, but could be taken to be that part of the original PKA energy, which is transferred to the atoms of the lattice (rather than the electrons) in slowing down. In reality, collisions of the PKA with atoms compete with collisions with electrons. But the processes can be treated as independent events. Nevertheless, the expression for $v(T)$ needs to be reformulated.

In 1975, Norgett, Robinson, and Torrens [17] proposed a model to calculate the number of displacements per PKA according to:

$$v(T) = \frac{\kappa E_D}{2E_d} = \frac{\kappa(T - \eta)}{2E_d}, \tag{2.50}$$

where $T$ is the total energy of the PKA, $\eta$ is the energy lost in the cascade by electron excitation, and $E_D$ is the energy available to generate atomic displacements by elastic collisions and is known as the *damage energy*. The displacement efficiency, $\kappa$, is 0.8 and is independent of $M_2$, $T$, and temperature. The quantity $E_D$ is defined by:

$$E_D = \frac{T}{[1 + k_N g(\in)]}, \tag{2.51}$$

and inelastic energy loss is calculated according to the method of Lindhard using a numerical approximation to the universal function, $g(\in)$:

$$g(\in) = 3.4008 \in^{1/6} + 0.40244 \in^{3/4} + \in$$
$$k_N = 0.1337 Z_1^{1/6} \left(\frac{Z_1}{A_1}\right)^{1/2}, \tag{2.52}$$

where $\in$ is the reduced energy given by:
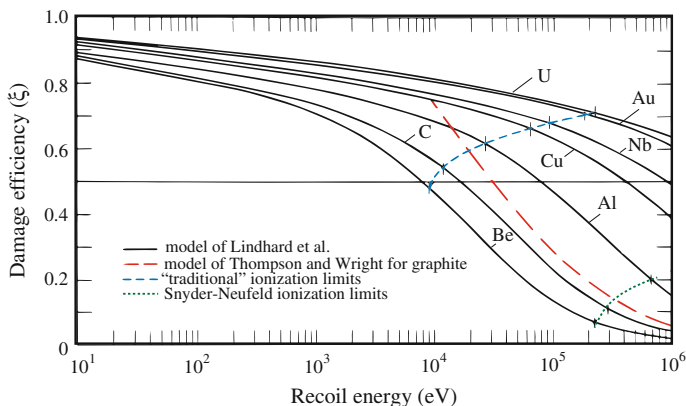
$$\in = \left(\frac{A_2 T}{A_1 + A_2}\right) \left(\frac{a}{Z_1 Z_2 \varepsilon^2}\right)$$
$$a = \left(\frac{9\pi^2}{128}\right)^{1/3} a_0 (Z_1^{2/3} + Z_2^{2/3})^{-1/2}, \tag{2.53}$$

$a_0$ is the Bohr radius, and $\varepsilon$ is the unit electronic charge. If $E_d \sim 40$ eV, then $v = 10E_D$, where $E_D$ is in keV.

The displacement function can also be written as the Kinchin–Pease result modified by a damage energy function, $\xi(T)$, given by:

$$v(T) = \xi(T) \left(\frac{T}{2E_d}\right), \tag{2.54}$$

**Fig. 2.10** The effect of electronic energy losses on the energy available for atomic displacements (after [16])

where

$$\xi(\in) = \cfrac{1}{1+0.1337 Z_1^{1/6}\left(\cfrac{Z_1}{A_1}\right)^{1/2}\left(3.4008\in^{1/6}+0.40244\in^{3/4}+\in\right)}, \quad (2.55)$$

and giving the same result as in Eq. (2.50) except for the exclusion of the displacement efficiency, $\kappa$. Figure 2.10 shows the effect of accounting for damage efficiency in the Kinchin–Pease result. Note that the function approaches 1.0 as the recoil energy is reduced. As energy increases, the damage efficiency drops faster for light materials.

## 2.2.4 Effects of Crystallinity

The analysis thus far has assumed that the cascade occurs in a solid composed of a random array of atoms. However, when the order of a crystal structure is imposed (Assumption 6), two important effects occur that can alter the number of displacements produced by a PKA; focusing and channeling. *Focusing* is the transfer of energy and/or atoms by near head-on collisions along a row of atoms. *Channeling* is the long-range displacement of atoms along open directions (channels) in a crystal structure in which an atom travels by making glancing collisions with the walls of the channel which are just rows of atoms. Both processes can result in long-range transport of interstitials away from the initial PKA or the cascade. Both processes also reduce the number of displacements per PKA, $\nu(T)$, as calculated from the simple Kinchin–Pease model.

**Focusing**

The effects of focusing were first seen in the directional dependence of the threshold energy, $E_d$. In an fcc lattice, for example, displacements occur in the $\langle 100 \rangle$ and $\langle 110 \rangle$ directions with the lowest energy transfer of any crystalline direction. Since the direction of the primary knock-on is random, focusing must be possible for a sizable range of polar angles off the close-packed direction. If exact head-on collision were required to produce a linear collision chain, the phenomenon would be of little practical significance since this probability is extremely low.

Focusing along an atomic row can be analyzed using the hard sphere approximation. The distance between atoms along a particular crystallographic direction is denoted by $D$. Figure 2.11 shows two atoms of such a row in which a collision sequence is initiated by the atom which was initially centered at $A$. This atom receives energy $T$ and moves off at an angle $\theta_0$ to the atomic row. The dashed circle shows the atom position at the instant it strikes the next atom in the row. The radius of the colliding sphere, $R$, is obtained from the Born–Mayer potential. The impact transfers some of $T$ to the second atom, which then moves off in the direction of the line joining $P$ and $B$ at an angle $\theta_1$ to the row. From Fig. 2.11, we can also show that:

$$\overline{AP} \sin \theta_0 = \overline{PB} \sin \theta_1. \tag{2.56}$$

If $\theta_0$ and $\theta_1$ are small, Eq. (2.56) can be approximated by:

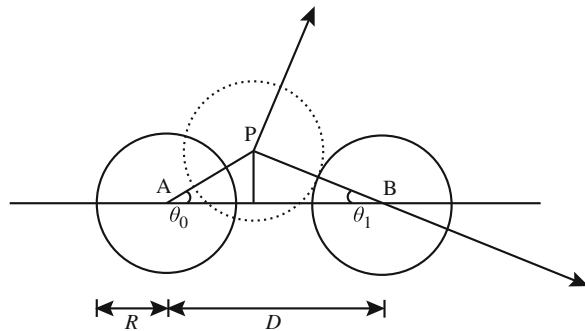$$\overline{AP}\theta_0 \approx \overline{PB}\theta_1, \tag{2.57}$$

and if $\theta_0$ and $\theta_1$ are very small, then:

$$\overline{AP} \approx \overline{AB} - \overline{PB} = D - 2R, \quad \text{and since } \overline{PB} = 2R$$
$$(D - 2R)\theta_0 = 2R\theta_1, \tag{2.58}$$

and

$$\theta_0(D - 2R) = \theta_1(2R). \tag{2.59}$$



**Fig. 2.11** The simple focusing effect assuming hard sphere collisions

If we further define a focusing parameter:

$$f \equiv \theta_1/\theta_0, \tag{2.60}$$

then by Eq. (2.59):

$$f = \frac{D}{2R} - 1. \tag{2.61}$$

This permits us to write the following inequalities:

$$\begin{aligned}&\text{for } f > 1, D > 4R \text{ and } |\theta_0| < |\theta_1| \\ &\text{for } f < 1, D < 4R \text{ and } |\theta_0| > |\theta_1|.\end{aligned} \tag{2.62}$$

Considering further collisions, by the time the momentum pulse reaches atom $n$, the relation between angles is given by:

$$\begin{aligned}\theta_n &= f\theta_{n-1} \\ &= f^2\theta_{n-2} \\ &= f^3\theta_{n-3} \\ &\vdots \\ &= f^n\theta_0 = \left(\frac{D}{2R} - 1\right)^n \theta_0,\end{aligned} \tag{2.63}$$

or finally:

$$\theta_n = (f)^n\theta_0 = \left(\frac{D}{2R} - 1\right)^n \theta_0. \tag{2.64}$$

This last relation shows that if $D > 4R$, the focusing parameter $f$ is greater than unity so that the angles $\theta_n$ will increase in successive collisions. Conversely, if $D < 4R$, $f$ is less than unity and the angles $\theta_n$ converges to zero.

A set of conditions also exist under which the scattering angle $\theta_n$ will neither diverge nor converge after successive collisions. These are the conditions for critical focusing ($\theta_n = \theta_{n+1} = \ldots$) which can be determined as follows. The recoil angle of atom $B$ can be related to the initial direction of atom $A$ by applying the law of sines to triangle $\overline{APB}$:

$$\frac{\sin(\pi - \theta_0 - \theta_1)}{\sin \theta_0} = \frac{D}{2R}, \tag{2.65}$$

which simplifies to:

$$\frac{\sin(\theta_0 + \theta_1)}{\sin \theta_0} = \frac{D}{2R}. \tag{2.66}$$

The condition for critical focusing is $\theta_1 = \theta_0$. Applying this equality in Eq. (2.66) gives:

$$\frac{\sin 2\theta_0}{\sin \theta_0} = 2\cos \theta_0 = \frac{D}{2R}, \tag{2.67}$$

and

$$\cos \theta_0 = \cos \theta_c = \frac{D}{4R}, \tag{2.68}$$

or focusing will occur when $\cos \theta_0 \leq \dfrac{D}{4R}$ and:

$$\cos \theta_c = \frac{D}{4R}. \tag{2.69}$$

Equation (2.60) also shows that focusing of momentum is favored along rows of atoms in the $\langle hkl \rangle$ directions for which the separation distance $D^{hkl}$ is a minimum, or the close-packed directions.

   If we treat the atoms as having an energy-dependent radius, we can determine the maximum possible energy for focusing at any given collision angle. The key is to allow the potential between atoms to vary with separation. The critical focusing energy, $E_{fc}^{hkl}$, is defined as that energy below which $f < 1$ and $D < 4R$, and focusing is possible. In the hard sphere model, the relation between kinetic energy, $E$, and potential energy $V(r)$ for a head-on collision is given by Eq. (1.80) as $V(2R) = \frac{1}{2}E$. If $V(r)$ is described by the Born–Mayer potential, Eq. (1.47), then $V(r) = A \exp(-Br)$, and:

$$E = 2A \exp(-2R/B). \tag{2.70}$$

For a head-on collision, $\theta_c = 0$, so $\cos \theta_c = \dfrac{D}{4R} = 1$, and we have:

$$E_{fc} = 2A \exp\left(\frac{-D}{2B}\right). \tag{2.71}$$

This means that any angle greater than zero will result in defocusing for $E \geq E_{fc}$ or that focusing at an energy $E_{fc}$ can only occur for $\theta = 0°$. Clearly then, the critical focusing angle depends on the energy of the projectile. The relation between angle and energy is developed by writing the expression for $E_{fc}$ in terms of $D$:

$$D = 2B \ln\left(\frac{2A}{E_{\text{fc}}}\right). \tag{2.72}$$

Now, for any atom of energy $T$ reaching a separation of $4R$:

$$4R = 2B \ln\left(\frac{2A}{T}\right). \tag{2.73}$$

Combining these equations gives:

$$\frac{D}{4R} = \cos\theta_{\text{c}} = \frac{\ln(2A/E_{\text{fc}})}{\ln(2A/T)}, \quad T < E_{\text{fc}}. \tag{2.74}$$

Note that the condition of critical focusing can be expressed in two ways:

1. $E_{\text{fc}} = 2A \exp\left(\frac{-D}{2B}\right)$ : This condition gives the energy $E_{\text{fc}}$ for which focusing occurs for a head-on collision ($\theta_{\text{c}} = 0$).

2. $\cos\theta_{\text{c}} = \frac{\ln(2A/E_{\text{fc}})}{\ln(2A/T)}$ : This condition gives the maximum angular deviation from a head-on collision $\theta_{\text{c}}$, at which a PKA of energy $T$ can initiate a focused sequence.

From the first expression, it should be apparent that focusing is a function of crystallographic direction since $D$ is a function of crystal structure. That is,

$$E_{\text{f}}^{hkl} = 2A \exp\left(\frac{-D^{hkl}}{2B}\right). \tag{2.75}$$

For example, in the fcc lattice, we have:

$$D^{\langle 100\rangle} = a$$

$$D^{\langle 110\rangle} = \frac{\sqrt{2}}{2}a$$

$$D^{\langle 111\rangle} = \sqrt{3}a$$

therefore, since $D^{\langle 110\rangle} < D^{\langle 100\rangle} < D^{\langle 111\rangle}$, we have $E_{\text{f}}^{\langle 110\rangle} > E_{\text{f}}^{\langle 100\rangle} > E_{\text{f}}^{\langle 111\rangle}$.

Typical values for $E_{\text{f}}^{\langle 110\rangle}$ are 80 eV in copper and 600 eV for gold. In any case, $E_{\text{f}}$ is much less than initial PKA energies.

From the preceding discussion, it should be apparent that focusing is only applicable if a scattered atom is within an angle $\theta_{\text{c}}$ of an atomic row. Then, a focused sequence can result. It is therefore important to determine the probability that the initial direction of a struck atom is within a cone of apex $\theta_{\text{c}}$ about an atomic row.

For a random starting direction, the probability of generating a focused collision sequence at energy $T$ is as follows

$$P_f(T) = \frac{\theta_c^2}{4}. \tag{2.76}$$

Expanding $\cos \theta_c$ in Eq. (2.69) gives:

$1 - \frac{1}{2}\theta_c^2 \approx \frac{D}{4R}$, for small $\theta_c$. Substituting from Eq. (2.76) gives:

$$P_f(T) = \frac{1}{2}\left(1 - \frac{D}{4R}\right), \tag{2.77}$$

or

$$\begin{aligned}P_f(T) &= \frac{1}{2}\left[1 - \frac{\ln(2A/E_{fc})}{\ln(2A/T)}\right]\\ &= \frac{1}{2}\left[\frac{\ln(2T/E_{fc})}{\ln(E_{fc}/2A) + \ln(T/E_{fc})}\right].\end{aligned} \tag{2.78}$$

Since $E_{fc}/2A \ll 1$ and $T/E_{fc} \sim 1$, then:

$$\begin{aligned}P_f(T) &= \frac{1}{2}\frac{\ln(T/E_{fc})}{\ln(E_{fc}/A)} \quad T < E_{fc}\\ &= 0 \quad T > E_{fc}\end{aligned} \tag{2.79}$$

For $n$ equivalent directions in the crystal:

$$P_f(T) = n\frac{\ln(T/E_{fc})}{\ln(E_{fc}/A)}. \tag{2.80}$$

For example, in copper, $E_{fc} \sim 80$ eV, and for $A \sim 20{,}000$ eV, $P_f(60 \text{ eV}) \sim 0.026n$. For $n = 12$, then $P_f \sim 0.3$ or 30 %. Focusing refers to the transfer of energy by elastic collisions along a line, but without involving the transfer of mass. We will next discuss replacement collisions in which both energy and mass are transferred.

### Replacement Collisions

In addition to energy transfer, mass can be transferred by replacement of the struck atom with the striking atom if the center of the first atom moves beyond the midpoint of the two atoms as they reside in the lattice. In our analysis of focusing, we assumed hard sphere collisions. However, if we assume that there is a softness to the atom, three things occur:

1. The hard sphere model overestimates the angle of scattering for a particular impact parameter, and hence, the amount of focusing must be overestimated.
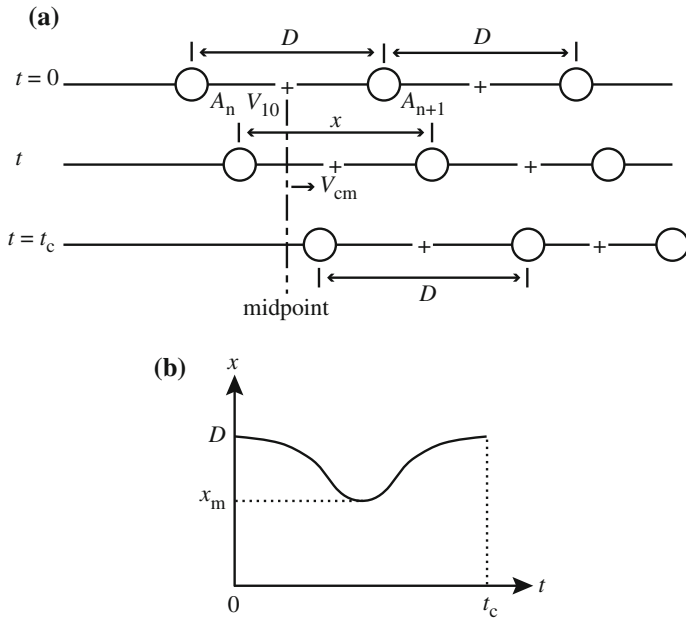
**Fig. 2.12** Head-on collisions in a focused chain when the interaction potential acts continuously during the collision. (**a**) Atom positions during the collision initiated by the atom on the *left*. (**b**) Separation of atoms $A_n$ and $A_{n+1}$ during the collision (after [5])

2. Atoms in the row feel the influence of the oncoming disturbance long before it gets there so the atom is already moving. Since $D$ is decreased, focusing is enhanced.
3. Replacement becomes possible.

Referring to Fig. 2.12, as the collision proceeds, the distance $x$ between atoms $A_n$ and $A_{n+1}$ decreases continuously. The velocity of the center of mass (CM) is as follows:

$$V_{CM} = \left(\frac{M_1}{M_1 + M_2}\right)v_1 + \left(\frac{M_2}{M_1 + M_2}\right)v_2,$$

where $v_1$ and $v_2$ are in the laboratory system. The relative speed, defined by $g = v_1 - v_2$, gives:

$$v_1 = V_{CM} + \left(\frac{M_2}{M_1 + M_2}\right)g$$

$$v_2 = V_{CM} + \left(\frac{M_1}{M_1 + M_2}\right)g,$$

and the total kinetic energy of the two particles is as follows:

$$KE = 1/2M_1v_1^2 + 1/2M_2v_2^2,$$

and in terms of $g$ and $V_{CM}$ is as follows

$$KE = 1/2(M_1 + M_2)V_{CM}^2 + 1/2\mu g^2,$$

where $\mu$ is the reduced mass $= \left(\dfrac{M_1 M_2}{M_1 + M_2}\right)$. The total kinetic energy is divided into two parts: one due to the motion of the system and another due to the relative motion of the two particles. Conservation of total energy is given as $E_r + V(x) = E_{r0}$, where $V(x)$ is the potential energy at a head-on separation distance of $x$, $E_{r0}$ is the relative kinetic energy at infinite (initial) separation, and $E_r$ is the relative kinetic energy at any point. Rewriting the kinetic energy in terms of $g$ gives:

$$\frac{1}{2}\mu g^2 + V(x) = \frac{1}{2}\mu g_0^2$$

and

$$g_0 = v_{10},$$

where $g_0$ is the initial speed. This equation should be recognizable from our earlier analysis in Chap. 1, Sect. 1.2.2. Recall that at $x = x_{min}$, $V(x_{min}) = 1/2\mu g_0^2$, and for $M_1 = M_2$, then $g_0 = v_{10}$ and $V = E/2$.

We also assume that the interaction energy at the initial separation is $V(D) \ll \frac{1}{2}\mu g_0^2$. The time rate of change of the separation distance is equal to the relative speed:

$$\frac{dx}{dt} = -g. \tag{2.81}$$

Taking the collision time as twice the time needed to reach the distance of closest approach:

$$t_c = -2\int_D^{x_m} \frac{dx}{g} = -2\int_{V(D)}^{V(x_m)} \frac{dV}{g\,dV/dx}, \tag{2.82}$$

where $x_m$ is the distance of closest approach.

Since $V(x) = A\,\exp(-x/B)$, then:

$$\frac{dV}{dx} = -\frac{A}{B}\exp(-x/B) = -\frac{V}{B}, \tag{2.83}$$

and:

$$g = \left\{ \left[ \frac{1}{2} \mu g_0^2 - V(x) \right] \frac{4}{M} \right\}^{1/2}$$

$$= \left\{ \left[ \frac{E}{2} - V \right] \frac{4}{M} \right\}^{1/2} \tag{2.84}$$

$$= 2 \left\{ \frac{E}{2M} - \frac{V}{M} \right\}^{1/2},$$

where $\mu = M/2$ for like atoms and $1/2\mu g_0^2 = 1/4 M v_{10}^2 = E/2$. Substitution of Eqs. (2.83) and (2.84) into Eq. (2.82) yields:

$$t_c = B \left( \frac{2M}{E} \right)^{1/2} \int_{V(D)}^{E/2} \frac{dV}{V(1 - 2V/E)^{1/2}} \tag{2.85}$$

$$= 2B \left( \frac{2M}{E} \right)^{1/2} \tanh^{-1} \left[ 1 - \frac{2V(D)}{E} \right]^{1/2}. \tag{2.86}$$

Note that the definition of a hard sphere radius has been used for the upper limit, i.e., $x_m$ is taken to be $2R(E)$. For $V(D)/E \ll 1$,

$$t_c = B \left( \frac{2M}{E} \right)^{1/2} \ln \left[ \frac{2E}{V(D)} \right]. \tag{2.87}$$

Since the speed of the center of mass is $\frac{v_{10}}{2} = \left( \frac{E}{2M} \right)^{1/2}$, the distance moved by the CM during the collision time, $t_c$, is as follows:
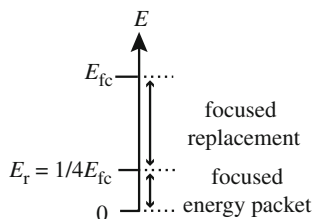
$$x = t_c \left( \frac{E}{2M} \right)^{1/2}. \tag{2.88}$$

If $x > D/2$, atom $A_n$ will end up to the right of the initial halfway point and replacement will occur, and $A_n$ will occupy the lattice site occupied by atom $A_{n+1}$. Relating the distance $x$ to energy by substituting for $t_c$ from Eq. (2.87) into Eq. (2.88) gives:

$$\frac{x}{B} = \ln \left( \frac{2E_r}{V(D)} \right). \tag{2.89}$$

For $x = D/2$:

$$\exp \left( \frac{D}{2B} \right) = \frac{2E_r}{A \exp(-D/B)},$$

**Fig. 2.13** Energy scale for focused energy transfer and focused replacement sequence

and the replacement energy becomes:

$$E_r = \frac{A}{2} \exp\left(\frac{-D}{2B}\right). \tag{2.90}$$

According to the above arguments, and comparing to Eq. (2.71), focused replacement is possible when the energy transported in the collision chain satisfies:

$$E > E_r = \frac{1}{2} A \exp\left(\frac{-D}{2B}\right) = \frac{1}{4} E_{fc}. \tag{2.91}$$

Therefore, we get focused replacement, or:

$E_{fc}/4 < T < E_{fc}$   focused replacement
$T < E_{fc}/4$            focused momentum/energy packet

Hence, mass transfer can occur when $E$ is between $E_r = E_{fc}/4$ and $E_{fc}$, which from our previous example is about the same or slightly less than the displacement energy, $E_d$. Figure 2.13 shows where focusing and replacement collisions fall on the energy spectrum of the PKA.

**Assisted Focusing**

In our analysis of focusing, we have not accounted for the effects of surrounding atoms or nearest neighbors. Due to their repulsion of the moving atom, they tend to act as a lens and aid in the focusing process. The net result of this assisted focusing is to increase the critical energy for focusing, $E_{fc}$, rendering focusing more probable. Second, the ring of atoms surrounding a focusing event also tends to dissipate energy by glancing collisions. This effect is augmented by the vibrational motion of the atom rings, which can be increased with temperature. The length of the replacement chain and the number of collisions in the chain decrease as the temperature increases. The increased motion of the surrounding atoms increases the energy loss from the collision sequence. Other effects that destroy the sequence are alloying elements and defects such as interstitials, vacancies, and dislocations. Figure 2.14 shows the number of collisions in a focused chain of initial energy $E$ in room temperature copper along with the focusing probability. Table 2.3 from Chadderton [18] gives the focusing and replacement energies in various directions in fcc and bcc lattices as

**Fig. 2.14** Length and probability of the collision chain in a <110> collision sequence in copper at room temperature (after [5])
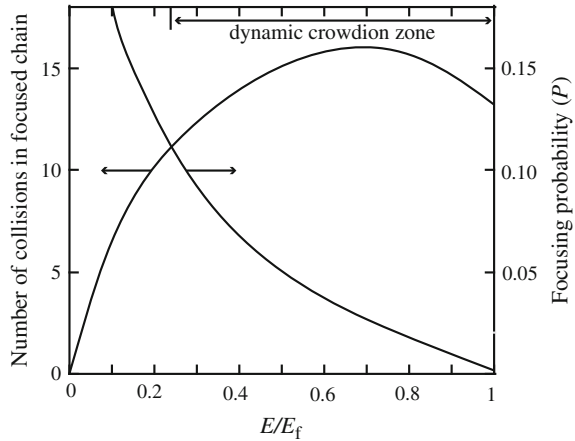


**Table 2.3** (**a**) Equations for $E_{\mathrm{fc}}^{hkl}$ in the fcc and bcc lattices considering assisted focusing (after [18]). (**b**) Equations for replacement energies ($E_{\mathrm{r}}^{hkl}$) in the fcc and bcc lattices (after [18])

(a)

| $\langle hkl \rangle$ | Face-centered cubic | Body-centered cubic |
|---|---|---|
| $\langle 100 \rangle$ | $\dfrac{A(D^{110})^2}{2B^2}\exp\left(-\dfrac{D^{110}}{4B}\right)^{\uparrow}$ | $2A\exp\left(-\dfrac{D^{111}}{B\sqrt{3}}\right)$ |
| $\langle 110 \rangle$ | $2A\exp\left(-\dfrac{D^{110}}{2B}\right)$ | $\dfrac{4\sqrt{2}(D^{111})^2A}{15B^2}\exp\left(-\dfrac{D^{111}\sqrt{5}}{2\sqrt{3}B}\right)^{\uparrow\uparrow}$ |
| $\langle 111 \rangle$ | $\left(\dfrac{6}{19}\right)^{1/2}\dfrac{A(D^{110})^2}{B^2}\exp\left(-\dfrac{D^{110}}{2B}\left(\dfrac{19}{12}\right)^{1/2}\right)^{\uparrow}$ | $2A\exp\left(-\dfrac{D^{111}}{2B}\right)$ |

(b)

| $\langle hkl \rangle$ | Face-centered cubic | Body-centered cubic |
|---|---|---|
| $\langle 100 \rangle$ | $5A\exp\left(-\dfrac{D^{110}}{D\sqrt{2}}\right)$ | $\dfrac{A}{2}\exp\left(-\dfrac{D^{100}}{2B}\right)$ |
| $\langle 110 \rangle$ | $\dfrac{A}{2}\exp\left(-\dfrac{D^{110}}{2B}\right)$ | $3A\exp\left(-\dfrac{D^{110}}{2B}\right)$ |
| $\langle 111 \rangle$ | $4A\exp\left(-\dfrac{D^{110}}{B\sqrt{3}}\right)$ | $2A\exp\left(-\dfrac{D^{111}}{2B}\right)$ |

$\uparrow$ In the (110) plane only
$\uparrow\uparrow$ Assisted focusing

modified by surrounding atoms (assisted focusing). Note that in all cases, the focusing energies are larger when the surrounding atoms aid in the focusing process.

**Channeling**

Channeling is the long distance displacement of energetic knock-on atoms down an open direction in the crystal lattice. Figure 2.15a shows a schematic of an atom spiraling down an open channel in a crystal lattice, and Fig. 2.15b shows axial and
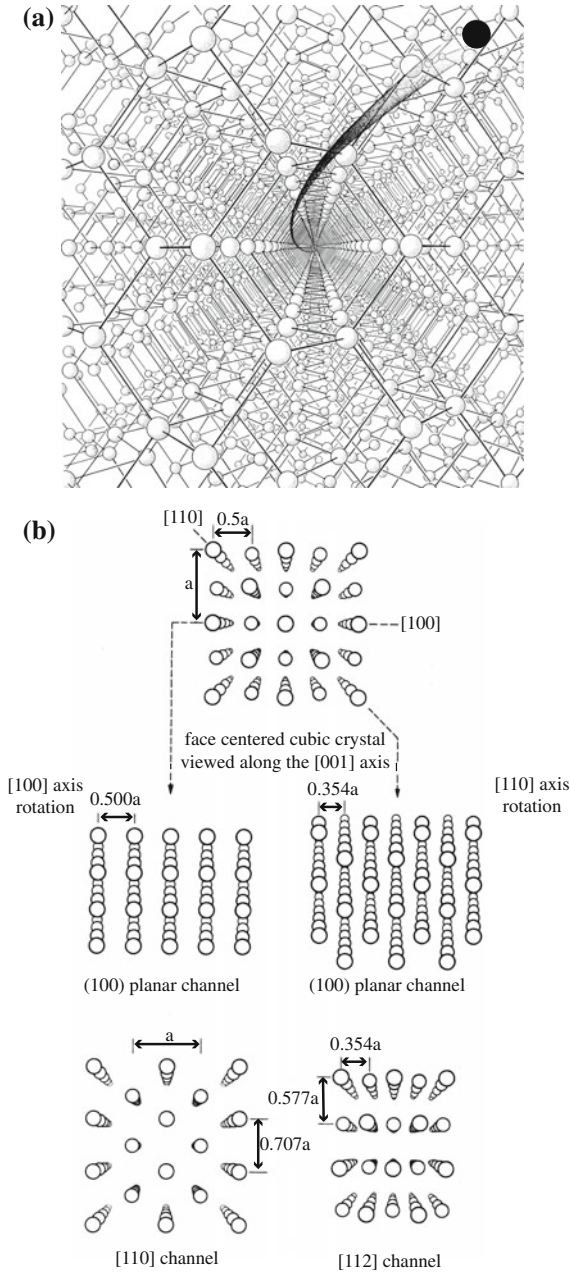
**Fig. 2.15** (**a**) Schematic of an atom moving in a channel in a crystal lattice (after [19]), and (**b**) axial and planar channels in the fcc lattice (after [20])

**Fig. 2.16** Trajectory of a channeled atom (after [5])
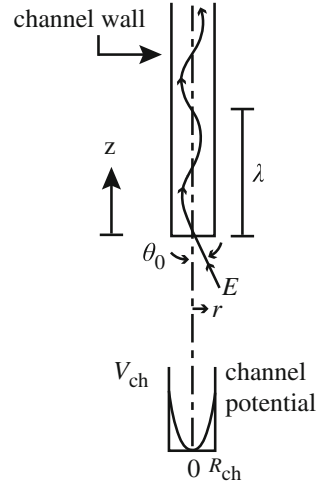
planar channels along specific crystallographic directions in the fcc lattice. The walls of the passageway consist of atomic rows. If the rows surrounding the channel are close-packed, discrete repulsive forces between atoms are "smeared out" and the atom appears to be traveling in a long cylindrical tube with radius $R_{ch}$. The value of $R_{ch}$ can be determined by equating $\pi R_{ch}^2$ with the cross-sectional area of the channel. If the amplitude of the lateral oscillations of the moving atom is small compared to $R_{ch}$, the potential well provided by the channel wall is roughly parabolic in the direction transverse to the channel axis.

The interaction of the moving atom with a channel wall (Fig. 2.16) can be described by a harmonic channel potential:

$$V_{ch}(r) = kr^2, \tag{2.92}$$

where $r$ is the lateral distance from the axis, and $k$ is the force constant that depends on the potential function describing atom–atom repulsion and channel dimension $R_{ch}$. Using the Born–Mayer potential to describe atom–atom interactions in this energy regime, $k$ becomes:

$$k = \frac{A}{DB} \left( \frac{2\pi R_{ch}}{B} \right) \exp\left( \frac{-R_{ch}}{B} \right), \tag{2.93}$$

where $D$ is the atom spacing in the rows forming the channels. Moving atoms enter the channel with a velocity component along the channel axis (Fig. 2.16) given by:

$$V_{z0} = \left( \frac{2E}{M} \right)^{1/2} \cos \theta_0, \tag{2.94}$$

where $(2E/M)^{1/2} = V_0$. The axial velocity is gradually reduced by inelastic energy loss to the electron cloud. The moving atom undergoes simple harmonic motion in the $r$ direction with period $\tau$ given by:

$$\tau = 2\pi \left(\frac{M}{2k}\right)^{1/2}, \tag{2.95}$$

and the initial wavelength of the oscillation is equal to $V_{z0}\tau$ for $\theta_0 = 0$ or:

$$\lambda = 2\pi \left(\frac{E}{k}\right)^{1/2}. \tag{2.96}$$

The amplitude of lateral oscillation is determined by the injection angle, $\theta_0$, and the kinetic energy of the injected atom, $E$. The $r$ component of the atom velocity as it enters the channel is as follows:

$$V_{r0} = \left(\frac{2E}{M}\right)^{1/2} \sin \theta_0 \cong \left(\frac{2E}{M}\right)^{1/2} \theta_0. \tag{2.97}$$

So the radial component of the kinetic energy is $E\theta_0^2$, which is equal to the potential energy at the transverse amplitude, $kr_{max}^2$. Equating kinetic and potential energies and solving for $r_{max}$ gives:

$$r_{max} = \left(\frac{E}{k}\right)^{1/2} \theta_0, \tag{2.98}$$

and the trajectory of the channeled atom is as follows:

$$r = \theta_0 \left(\frac{E}{k}\right)^{1/2} \sin \left[\left(\frac{k}{E}\right)^{1/2} z\right]. \tag{2.99}$$

The critical angle below which channeling can occur, $\theta_{ch}$, is obtained by equating the transverse amplitude, $r_{max}$, and the channel radius, $R_{ch}$:

$$\theta_{ch} = R_{ch} \left(\frac{k}{E}\right)^{1/2}. \tag{2.100}$$

Note that $\theta_{ch}$ decreases as $E$ increases, as expected. When the mean free path between collisions is of the order of a few atom spacings, large-angle collisions become probable and channeling dissipates. The channeling probability is difficult to determine since an atom must be knocked into the channel, but there are no atoms near the channel axis. The event probably starts with an impact on an atom forming the channel wall. If the entrance angle is small enough, it may begin to channel.

There is no upper limit on energy for channeling. Instead, $\theta_{ch}$ just becomes smaller as $E$ increases. The minimum channeling energy occurs when the wavelength is $\sim nD$ or a few atom spacings ($n \sim 2$). Essentially, there develops a resonance between impulses from channel walls and transverse oscillations. The trajectory terminates in a violent collision. Recall that our treatment is only valid if $\lambda \gg D$. Solving for $E$ in Eq. (2.96) and letting $\lambda = 2D$ yield $E_{ch} \sim 0.1\,kD^2$. For copper, $E_{ch}$ is about 300 eV. $E_{ch}$ is larger for large mass because $k$ increases with mass. Channeling is a high-energy phenomenon and is most significant for light atoms, while focusing is a low-energy phenomenon that is most significant for heavy atoms.

**Effect of Focusing and Channeling on Displacements**

The probability of a crystal effect is a function of recoil energy. $P(T)$ is used for either $P_f$ or $P_{ch}$, but since $E_f \sim 100$ eV, $P_f$ is quite small. The equation governing cascade effects can be modified to account for crystal effects by modifying Eq. (2.14):

$$\nu(T) = P(T) + [1 - P(T)]\left[\frac{2E_d}{T} + \frac{2}{T}\int_{2E_d}^{T}\nu(\varepsilon)\,d\varepsilon\right]. \tag{2.101}$$

The first term on the right of Eq. (2.101) represents the lone displaced atom, which results if the PKA is channeled or focused on the first collision. The second term gives the number of displacements created by a PKA that makes an ordinary displacement on the first collision. Assuming $P \neq P(T)$, Eq. (2.101) is differentiated with respect $T$ to yield:

$$T\frac{d\nu}{dT} = (1 - 2P)\nu + P. \tag{2.102}$$

Integration gives

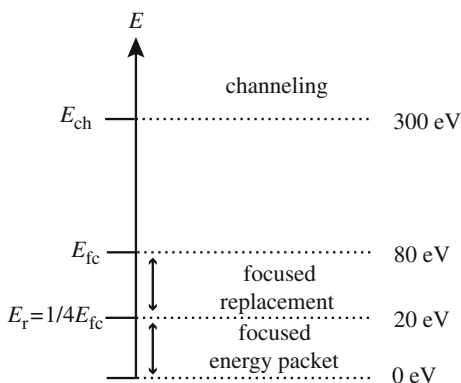$$\nu(T) = \frac{CT^{(1-2P)} - P}{1 - 2P}, \tag{2.103}$$

and the constant, $C$ can be found by substitution into Eq. (2.102):

$$C = \frac{1 - P}{(2E_d)^{(1-2P)}},$$

resulting in the final solution:

$$\nu(T) = \frac{1 - P}{1 - 2P}\left(\frac{T}{2E_d}\right)^{(1-2P)} - \frac{P}{1 - 2P}. \tag{2.104}$$

**Fig. 2.17** Energy scale showing focused energy transfer and focused replacement sequence and channeling

$E$

channeling

$E_{ch}$ ............................................................ 300 eV

$E_{fc}$ ............................................................ 80 eV

focused

replacement

$E_r = 1/4 E_{fc}$ ..................................................... 20 eV

focused

energy packet

............................................................ 0 eV

For small $P$, $v(T)$ can be approximated by:

$$v(T) = \left(\frac{T}{2E_d}\right)^{(1-2P)}. \tag{2.105}$$

It should be noted that the most important crystal effect is channeling, which is most important at high energies. For example, for $P = 7\%$, a 10 keV PKA in iron produces 100 displacements or about half the amount with $P = 0$. Figure 2.17 shows where channeling occurs on the PKA energy scale. Note that channeling is a high-energy phenomenon and that there is a gap between the replacement energy, below which replacements or focused energy transfer occurs, and the channeling energy, above which channeling occurs. Given the K–P model for displacement and the various modifications to the basic model, we now turn to the determination of the number of displaced atoms.

## 2.3   The Displacement Cross Section

The results of previous sections may now be used to define the displacement cross section as:

$$\sigma_D(E_i) = \int_{\check{T}}^{\hat{T}} v(T)\sigma\big(E_i, Q_j, T\big) \, dT, \tag{2.106}$$

where $v(T)$ is the number of displacements caused by a PKA of energy $T$, $\sigma(E_i, Q_j, T)$ is the general form of the energy transfer cross section, and $\check{T}$ and $\hat{T}$ are the minimum and maximum transfer energies. This quantity was first presented in Eq. (2.2) and gives the average number of displacements produced by an incoming neutron of energy $E_i$. We can apply this expression to the various regimes of scattering in order to determine their individual contributions to the total number of displacements.

We will first determine $\sigma_D(E_i)$ for each type of interaction using the basic K–P result and then go back and add in the modifications.

### 2.3.1 Elastic Scattering

Consider $\sigma_s(E_i, T)$ for elastic scattering. From Eq. (1.19),

$$\sigma_s(E_i, T) = \frac{4\pi}{\gamma E_i} \sigma_s(E_i, \phi).$$

In the case of isotropic scattering:

$$\sigma_s(E_i, \phi) = \frac{\sigma_s(E_i)}{4\pi}; \quad \sigma_s(E_i, T) = \frac{\sigma_s(E_i)}{\gamma E_i},$$

therefore,

$$\sigma_{Ds}(E_i) = \frac{\sigma_s(E_i)}{\gamma E_i} \int_{E_d}^{\gamma E_i} v(T)\mathrm{d}T. \tag{2.107}$$

Should we wish to consider anisotropic elastic scattering in systems such as fast reactors, the angular dependence of the elastic scattering cross section can be written in a series of Legendre polynomials:

$$\sigma_s(E_i, \phi) = \frac{\sigma_s(E_i)}{4\pi} \sum_{\ell=0}^{\infty} a_\ell(E_i)P_\ell(\cos \phi), \tag{2.108}$$

where $\sigma_s(E_i)$ is the total elastic scattering cross section for incident neutrons of energy $E_i$, $P_\ell$ is the $\ell$th Legendre polynomial, and values of $a_\ell$ are the energy-dependent coefficients of the cross section expansion. At neutron energies encountered in thermal or fast reactors, it is sufficient to retain only the first two terms, $\ell = 0$ and $\ell = 1$. Since $P_0 = 1$ and $P_1 = \cos \phi$:

$$\sigma_s(E_i, \phi) = \frac{\sigma_s(E_i)}{4\pi} [1 + a_1(E_i) \cos \phi]. \tag{2.109}$$

Also, given that $\cos \phi = 1 - 2T / \gamma E_i$ and substituting Eq. (2.109) into Eq. (2.106) gives:

$$\sigma_{Ds}(E_i) = \frac{\sigma_s(E_i)}{\gamma E_i} \int_{E_d}^{\gamma E_i} v(T) \left[1 + a_1(E_i) \left(1 - \frac{2T}{\gamma E_i}\right)\right] \mathrm{d}T. \tag{2.110}$$

## 2.3.2 Inelastic Scattering

Since inelastic scattering is isotropic in the center-of-mass system:

$$\sigma_{sj}(E_i, Q_j, \phi) = \frac{\sigma_{sj}(E_i, Q_j)}{4\pi}. \tag{2.111}$$

Equation (1.30) gives the energy transfer cross section for inelastic scattering in the resonance region as:

$$\sigma_{sj}(E_i, Q_j, T) = \frac{\sigma_{sj}(E_i, Q_j)}{\gamma E_i} \left[1 + \frac{Q_j}{E_i}\left(\frac{1+A}{A}\right)\right]^{-1/2},$$

so that

$$\sigma_{Dsj}(E_i) = \sum_j \frac{\sigma_{sj}(E_i, Q_j)}{\gamma E_i} \left[1 + \frac{Q_j}{E_i}\left(\frac{1+A}{A}\right)\right]^{-1/2} \int_{\check{T}_j}^{\hat{T}_j} v(T)dT, \tag{2.112}$$

where the minimum and maximum values of $T(E_i, Q_j, \phi)$ are given by Eq. (1.27), and setting $\cos\phi = -1$ and 1, respectively, gives:

$$\hat{T}_j = \frac{\gamma E_i}{2}\left[1 + \frac{1+A}{2A}\frac{Q_j}{E_i} + \left(1 + \frac{Q_j}{E_i}\frac{1+A}{A}\right)^{1/2}\right]$$

$$\check{T}_j = \frac{\gamma E_i}{2}\left[1 + \frac{1+A}{2A}\frac{Q_j}{E_i} - \left(1 + \frac{Q_j}{E_i}\frac{1+A}{A}\right)^{1/2}\right].$$

## 2.3.3 (n, 2n) and (n, γ) Displacements

The displacement cross section for (n, 2n) reactions can be written as:

$$\sigma_{D(n,2n)}(E_i) = \int_0^{E_i - E_m'} \sigma_{(n,2n)}(E_i, T)\frac{T}{2E_d}dT, \tag{2.113}$$

where $\sigma_{(n,\,2n)}(E_i, T)$ is given by Eq. (1.40).

The displacement cross section due to (n, γ) reactions can be written as:

$$\sigma_{D\gamma}(E_i) = \sigma_\gamma \int_0^{\hat{T}} \frac{T}{2E_d}dT. \tag{2.114}$$

However, since we have assumed that the lattice atom recoils with an average energy

$$\overline{T} = \frac{\hat{T}}{2} = \frac{E_\gamma^2}{4(A+1)c^2},$$

and that $E_\gamma$ for a given isotope is either known or can be measured, Eq. (2.114) can be simplified to:

$$\sigma_{D\gamma} = \sigma_\gamma \frac{\overline{T}}{2E_d} = \sigma_\gamma \frac{E_\gamma^2}{8E_d(A+1)c^2}. \tag{2.115}$$

The total displacement cross section due to these forms of neutron interaction then becomes:

$$
\begin{aligned}
\sigma_D(E_i) &= \sigma_{Ds}(E_i) + \sigma_{Dsj}(E_i) + \sigma_{D(n,2n)}(E_i) + \sigma_{D\gamma} \\
&= \frac{\sigma_s(E_i)}{\gamma E_i} \int_{E_d}^{\gamma E_i} \frac{T}{2E_d} \left[ 1 + a_1(E_i)\left( 1 - \frac{2T}{\gamma E_i} \right) \right] dT \\
&\quad + \sum_j \frac{\sigma_{sj}(E_i, Q_j)}{\gamma E_i} \left[ 1 + \frac{Q_j}{E_i}\left( \frac{1+A}{A} \right) \right]^{-1/2} \int_{\check{T}_j}^{\hat{T}_j} \frac{T}{2E_d} dT \\
&\quad + \int_0^{E_i - E'_m} \sigma_{(n,2n)}(E_i, T) \frac{T}{2E_d} dT \\
&\quad + \sigma_\gamma \frac{E_\gamma^2}{8E_d(A+1)c^2},
\end{aligned}
\tag{2.116}
$$

where the terms are for elastic scattering, inelastic scattering in the resonance region, (n, 2n) reactions and (n, $\gamma$) reactions, respectively.

## 2.3.4  Modifications to the K–P Model and Total Displacement Cross Section

The displacement cross section can be modified to account for the relaxation of the various assumptions made to the basic K–P model as in Sect. 2.2. These modifications are summarized in Table 2.4. Applying these correction terms to the basic K–P result by consolidating Assumptions 1 and 3 into a single constant $C'$ and using Eq. (2.104) for the effect of crystallinity transform Eq. (2.116) to read:

**Table 2.4**  Modifications to the displacement cross section

| Assumption | Correction to $\nu(T) = T/2E_d$ | Equation in text |
|---|---|---|
| 3: Loss of $E_d$ | $0.56\left(1 + \dfrac{T}{2E_d}\right)$ | Equation (2.31) |
| 4: Electronic energy loss cutoff | $\xi(T)\left(\dfrac{T}{2E_d}\right)$ | Equation (2.54) |
| 5: Realistic energy transfer cross section | $C\dfrac{T}{2E_d}, \quad 0.52 < C \le 1.22$ | Equation (2.33), (2.39) |
| 6: Crystallinity | $\dfrac{1-P}{1-2P}\left(\dfrac{T}{2E_d}\right)^{(1-2P)} - \dfrac{P}{1-2P}$ | Equation (2.104) |
| | $\sim \left(\dfrac{T}{2E_d}\right)^{(1-2P)}$ | Equation (2.105) |

$$
\begin{aligned}
\sigma_D = {} & \frac{\sigma_s(E_i)}{\gamma E_i} \int_{E_d}^{\gamma E_i} \left[ \frac{1-P}{1-2P}\left(C'\xi(T)\frac{T}{2E_d}\right)^{(1-2P)} - \frac{P}{1-2P} \right] \\
& \times \left[ 1 + a_1(E_i)\left(1 - \frac{2T}{\gamma E_i}\right) \right] dT \\
& + \sum_j \frac{\sigma_{sj}(E_i, Q_j)}{\gamma E_i} \left[ 1 + \frac{Q_j}{E_i}\left(\frac{1+A}{A}\right) \right]^{-1/2} \\
& \times \int_{\check{T}_j}^{\hat{T}_j} \left[ \frac{1-P}{1-2P}\left(C'\xi(T)\frac{T}{2E_d}\right)^{(1-2P)} - \frac{P}{1-2P} \right] dT \\
& + \int_0^{E_i - E_m'} \sigma_{(n,2n)}(E_i, T)\left[ \frac{1-P}{1-2P}\left(C'\xi(T)\frac{T}{2E_d}\right)^{(1-2P)} - \frac{P}{1-2P} \right] dT \\
& + \sigma_\gamma \left[ \frac{1-P}{1-2P}\left(C'\xi(T)\frac{E_\gamma^2}{8E_d(A+1)c^2}\right)^{1-2P} - \frac{P}{1-2P} \right].
\end{aligned}
$$

$$(2.117)$$

Using the more simplified expression for the effect of crystallinity, Eq. (2.104) reduces Eq. (2.117) to:
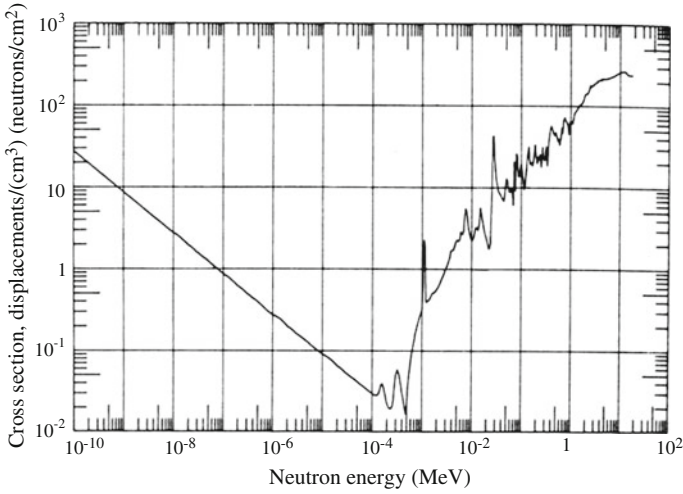
**Fig. 2.18** The displacement cross section for stainless steel based on a Lindhard model and ENDF/B scattering cross sections (after [21])

$$
\sigma_{\mathrm{D}} = \frac{\sigma_{\mathrm{s}}(E_{\mathrm{i}})}{\gamma E_{\mathrm{i}}} \int_{E_{\mathrm{d}}}^{\gamma E_{\mathrm{i}}} \left[ \left( C' \xi(T) \frac{T}{2E_{\mathrm{d}}} \right)^{(1-2P)} \right] \left[ 1 + a_1(E_{\mathrm{i}}) \left( 1 - \frac{2T}{\gamma E_{\mathrm{i}}} \right) \right] \mathrm{d}T
$$

$$
+ \sum_j \frac{\sigma_{sj}(E_{\mathrm{i}}, Q_j)}{\gamma E_{\mathrm{i}}} \left[ 1 + \frac{Q_j}{E_{\mathrm{i}}} \left( \frac{1+A}{A} \right) \right]^{-1/2} \int_{\check{T}_j}^{\hat{T}_j} \left( C' \xi(T) \frac{T}{2E_{\mathrm{d}}} \right)^{(1-2P)} \mathrm{d}T
$$

$$
+ \int_0^{E_{\mathrm{i}} - E_{\mathrm{m}}'} \sigma_{(\mathrm{n},2\mathrm{n})}(E_{\mathrm{i}}, T) \left( C' \xi(T) \frac{T}{2E_{\mathrm{d}}} \right)^{(1-2P)} \mathrm{d}T
$$

$$
+ \sigma_\gamma \left( C' \xi(T) \frac{E_\gamma^2}{8E_{\mathrm{d}}(A+1)c^2} \right)^{1-2P},
$$

$$
\tag{2.118}
$$

or,

$$
\sigma_{\mathrm{D}} = \sigma_{\mathrm{Ds}} + \sigma_{\mathrm{Di}} + \sigma_{\mathrm{D(n,2n)}} + \sigma_{\mathrm{D}\gamma}. \tag{2.119}
$$

The displacement cross section for stainless steel was calculated by Doran [21] using the energy partition theory of Lindhard and is shown in Fig. 2.18.

## 2.4  Displacement Rates

Recall that the displacement rate was given in Eq. (2.1) as:

$$R = \int_{\check{E}}^{\hat{E}} N\phi(E_i)\sigma_D(E_i)dE_i.$$

This is the displacement rate density or total number of displacements per unit volume per unit time [#/cm$^3$ s]. To get a rough estimate of the order of magnitude of this number, let us simplify the displacement cross sections as follows. Neglecting (n, 2n) and (n, $\gamma$) contributions to displacements, all modifications to the simple K–P displacement model (i.e., using $v(T) = T/2E_d$), and neglecting $E_d$ relative to $E_i$, the displacement cross section due to elastically and inelastically scattered neutrons only becomes:

$$\sigma_D(E_i) = \frac{\sigma_s(E_i)}{\gamma E_i} \int_{E_d}^{\gamma E_i} \frac{T}{2E_d}\left[1 + a_1(E_i)\left(1 - \frac{2T}{\gamma E_i}\right)\right]dT$$
$$+ \sum_j \frac{\sigma_{sj}(E_i, Q_j)}{\gamma E_i}\left[1 + \frac{Q_j}{E_i}\left(\frac{1+A}{A}\right)\right]^{-1/2} \int_{\check{T}_j}^{\hat{T}_j} \frac{T}{2E_d}dT. \tag{2.120}$$

Assuming that elastic scattering is isotropic ($a_1 = 0$), neglecting inelastic scattering and integrating between the limits $E_d$ and $\gamma E_i$ gives:

$$\sigma_D(E_i) = \frac{\sigma_s(E_i)}{\gamma E_i} \int_{E_d}^{\gamma E_i} \frac{T}{2E_d}dT, \tag{2.121}$$

and if $\gamma E_i > E_c$, then:

$$\sigma_D(E_i) = \frac{\sigma_s(E_i)}{\gamma E_i}\left[\int_{E_d}^{2E_d} dT + \int_{2E_d}^{E_c} \frac{T}{2E_d}dT + \int_{E_c}^{\gamma E_i} \frac{E_c}{2E_d}dT\right]$$
$$= \frac{\sigma_s(E_i)}{2\gamma E_i E_d}\left[\gamma E_i E_c - \frac{E_c^2}{2}\right]. \tag{2.122}$$

If we choose $\gamma E_i \sim E_c$, then we have:

$$\sigma_D(E_i) \approx \left(\frac{\gamma E_i}{4E_d}\right)\sigma_s(E_i), \tag{2.123}$$

and Eq. (2.1) becomes:

$$R_d = \frac{N\gamma}{4E_\mathrm{d}} \int_{E_{\mathrm{d}/\gamma}}^{\infty} \sigma_\mathrm{s}(E_\mathrm{i}) E_\mathrm{i} \phi(E_\mathrm{i}) \, \mathrm{d}E_\mathrm{i} \tag{2.124}$$

$$= N\sigma_\mathrm{s}\left(\frac{\gamma \bar{E}_\mathrm{i}}{4E_\mathrm{d}}\right)\phi, \tag{2.125}$$

where $\bar{E}_\mathrm{i}$ is an average neutron energy and $\phi$ is the total neutron flux above energy $E_\mathrm{d}/\gamma$, and the term in brackets is the number of displacements (Frenkel pairs) produced per neutron. The validity of assuming isotropic scattering and neglecting inelastic scattering is shown in Figs. 2.19 and 2.20. Essentially, both approximations are reasonable at energies below one to a few MeV.

*Example 2.1. Neutron irradiation of iron*
As an example, let us look at the damage caused by 0.5 MeV neutrons in Fe in a fast flux that may be representative of the core of a fast reactor:
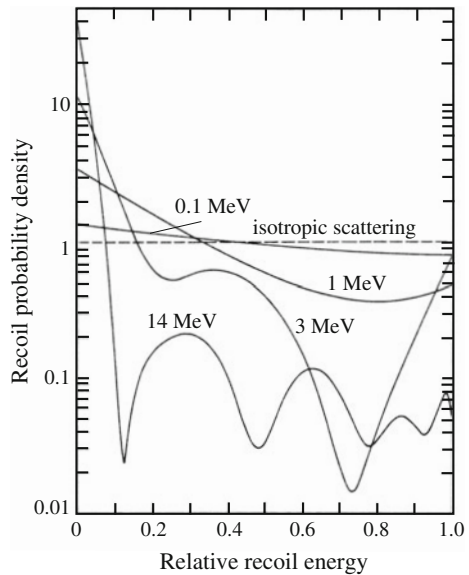
$N = 0.85 \times 10^{23}$ atoms/cm$^3$
$\sigma_\mathrm{s} = 3 \times 10^{-24}$ cm$^2$
$\phi = 10^{15}$ neutrons cm$^{-2}$s$^{-1}$
$\frac{\gamma \bar{E}_\mathrm{i}}{4E_\mathrm{d}} = 350$ displaced atoms/neutron

$R_d$ is $9 \times 10^{16}$ displaced atoms per cm$^3$ per second, or dividing $R_d$ by $N$ gives $\sim 10^{-6}$ dpa/s or about 32 dpa/year. This is equivalent to each atom being displaced from a normal lattice site once every 12 days.

**Fig. 2.19** Recoil energy spectra from the elastic scattering of fast neutrons using data from ENDF/B files (after [22])

**Fig. 2.20** Displacement cross section for nickel showing the elastic and inelastic components (after [21])
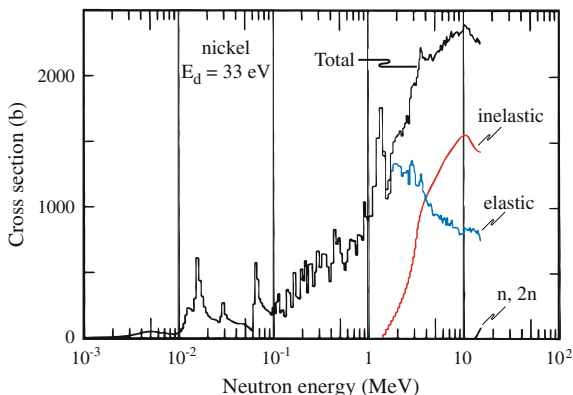
A second example can be worked for the displacement rate in the aluminum fuel plates in an MTR-type thermal neutron research reactor. In this case, we have:

$E_i \sim 0.5$ MeV
$N = 0.6 \times 10^{23}$ atoms/cm$^3$
$\sigma_s = 3 \times 10^{-24}$ cm$^2$
$\phi = 3 \times 10^{13}$ neutrons cm$^{-2}$s$^{-1}$
$\dfrac{\gamma E_i}{4 E_d} = 690$ displaced atoms/neutron

$R_d$ is $4 \times 10^{15}$ displaced atoms per cm$^3$ per second, or dividing $R_d$ by $N$ gives $\sim 7 \times 10^{-8}$ dpa/s or about 2 dpa/year. Note that even though the number of displacements per neutron is almost a factor of 2 higher in Al than in Fe, the damage rate is significantly lower because of the much lower fast flux in this type of reactor.

## 2.5   Correlation of Property Changes and Irradiation Dose

The ultimate objective of the calculation of $R_d$ is to provide a prediction of the extent of change of a particular property of the material under irradiation. The mechanical property may be yield strength, swelling, degree of embrittlement, etc. Recall in the introduction that the determination of the number of displaced atoms was motivated by the inability of particle fluence to account for property changes (see Fig. 1 in the Introduction). While an improvement over units of exposure such as neutron fluence, displacement rate alone cannot account for the macroscopic changes observed, and a semiempirical method of correlating damage with

macroscopic property changes has evolved known as the damage function method. In this method, the atom displacement rate is replaced with the change in some macroscopic property after a time t of irradiation. The displacement cross section is replaced by the damage function for the particular mechanical property, $G_i(E)$, hence:

$$\Delta P_{ij} = \int \int G_i(E)\phi_j(E,t)\, dE\, dt, \tag{2.126}$$

where $\Delta P_{ij}$ is the change in the property labeled by the index $i$, during an irradiation time of $t$ and in a neutron flux where $\phi_j(E,t)$ is the $j$th neutron differential spectrum. Assuming energy–time separability, $\phi_j(E,t) = \phi_j(E,)t$, then Eq. (2.126) can be rewritten as

$$\Delta P_{ij}^{(k)} = t \cdot \int G_i^{(k)}(E)\phi_j(E)\, dE, \tag{2.127}$$

where the superscript refers to the $k$th cycle of iteration.

The objective is to deduce a single function $G_i(E)$ from a set of measured $\Delta P_i$ values. Given $\Delta P_{ij}^{(k)}$ and $\phi_j(E)$ as input along with an initial approximation of $G_i(E)$ or $G_i^{(0)}(E)$, a computer code is used to generate iterative solutions $G_i^{(k)}(E)$. An appropriate solution is obtained when the standard deviation of the ratios of all measured-to-calculated values $\Delta P_{ij}/\Delta P_{ij}^{(k)}$ reaches a lower value that is consistent with experimental uncertainties. As it turns out, the resultant damage function is highly sensitive to the initial approximation as shown in Fig. 2.21. But note that since the shape of $G_i(E)$ is the same as the displacement function, it is clear that they are related. However, this result tells us that we cannot fully understand radiation effects by only calculating the number of displaced atoms. We cannot treat radiation effects as a black box. Rather, in order to understand the effect of the damage on the properties of the material, we must understand the fate of these defects after they are formed. This realization is reinforced by the property dependence on dose shown in Fig. 2.22. Note that for the three property changes, resistivity, radiation-induced segregation, and hardening, the functional dependence on dose is strikingly different between them. While property change certainly relates to displacement damage, the nature of the change is not uniform but varies considerably depending on the property measured. The next chapter explores the spatial and temporal distribution of radiation damage. But before we examine the damage zone in detail, let us complete our picture of the production of displacements by addressing the damage created by charged particles such as ions and electrons.
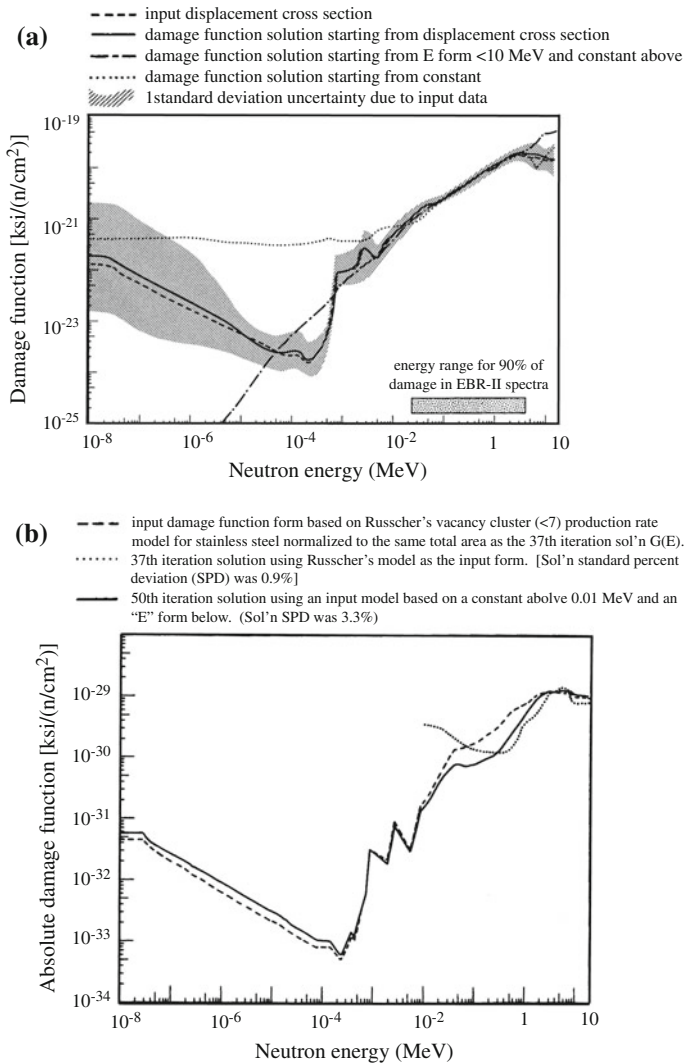
**Fig. 2.21** (**a**) 60 ksi yield strength damage function for 304 stainless steel irradiated and tested at 480 °C (after [23]) (**b**) Damage function for a $2.0 \times 10^{-8}$ psi$^{-1}$ $\bar{\varepsilon}/\bar{\sigma}$ property change for stainless steel (after [24])

## 2.6   Displacements from Charged Particle Irradiation

Displacement from charged particles differs from that due to neutrons because as they travel through the lattice, they lose energy via electronic excitation in addition to via elastic collisions. Figure 2.23 shows the trade-off in energy loss mechanism dominance with energy in the energy range of relevance for ion–solid interaction,
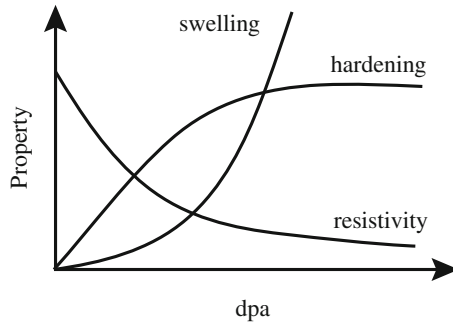
**Fig. 2.22**   Dose dependence of swelling, resistivity, and radiation-induced segregation
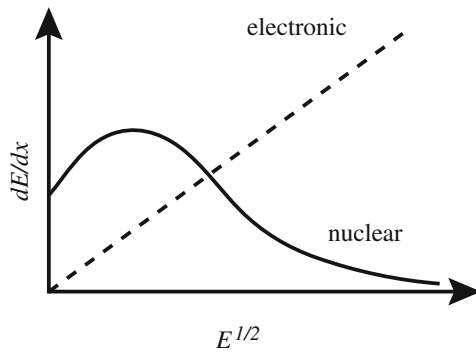


**Fig. 2.23**   Variation in nuclear and electronic stopping powers over the energy range of relevance to ion–solid interactions
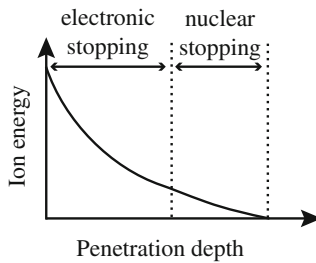


**Fig. 2.24**   Residual range of an ion incident on a target and the regimes of electronic and nuclear stopping dominance

and Fig. 2.24 shows the residual ion energy as a function of ion penetration depth. Note that electronic stopping will dominate at short depths, but elastic collisions will dominate near the end of range. An expression for the number of displacements from a charged particle can be derived from the analysis of energy lost from the

PKA by electronic excitation given in Sect. 2.2.3 and described by Eq. (2.40) through Eq. (2.49). Equation (2.44) describes the loss of energy to both atoms and electrons in the target by the PKA. We can revisit this analysis assuming that the particle we are tracking is the incident ion. As was done in Eq. (2.45), we can expand the terms for $v(T - \varepsilon_a)$ and $v(T - \varepsilon_e)$ in a Taylor series and truncate the series after the second term, giving:

$$v(T - \varepsilon_a) = v(T) - \frac{dv}{dT}\varepsilon_a,$$
$$v(T - \varepsilon_e) = v(T) - \frac{dv}{dT}\varepsilon_e,$$

(2.128)

and the integrals involving the terms $v(T - \varepsilon_a)$ and $v(T - \varepsilon_e)$ can both be written in the general form:

$$\int_0^{\varepsilon_{max}} v(T - \varepsilon)\sigma(T, \varepsilon)d\varepsilon = v(T)\int_0^{\varepsilon_{max}} \sigma(T, \varepsilon)d\varepsilon - \frac{dv}{dT}\int_0^{\varepsilon_{max}} \varepsilon\sigma(T, \varepsilon)\,d\varepsilon$$
$$= v(T)\sigma(T) - \frac{dv(T)}{dT}S(T),$$

(2.129)

where $S(T)$ is the stopping cross section. Since in this treatment, the ion is the incoming projectile, we will rewrite Eq. (2.129) using our established convention that the incoming particle is of energy $E_i$ and it transfers energy $T$ to the target atoms and electrons, and the maximum energy transfer is $\hat{T}$:

$$\int_0^{\hat{T}} v(E_i - T)\sigma(E_i, T)dT = v(E_i)\int_0^{\hat{T}} \sigma(E_i, T)dT - \frac{dv}{dE}\int_0^{\hat{T}} T\sigma(E_i, T)\,dT$$
$$= v(E_i)\sigma(E_i) - \frac{dv(E_i)}{dE}S(E_i),$$

(2.130)

where Eq. (1.79) is used to transform the integral of the differential energy transfer cross section, $\sigma(E_i, T)$, to the total collision cross section, $\sigma(E_i)$, and Eq. (1.129) is used to transform the integral of $T\sigma(E_i, T)$ into the stopping cross section $S(E_i)$. Applying the results of Eqs. (2.129) and (2.130) into Eq. (2.44) gives:

$$dv(E_i) = \frac{dE}{S(E_i)}\int_0^{\hat{T}} v(T)\sigma(E_i, T)\,dT.$$

(2.131)

Since we are concerned with the total number of displacements over the entire range of the ion rather than the specific number of displacements over a distance $dx$ of the sample, we can integrate Eq. (2.131) over the entire range of ion energy loss to obtain the number of displacements resulting from an incident ion with initial energy $E_i$:

$$v(E_i) = \int_0^{E_i} \frac{dE'}{S(E')} \int_{E_d}^{\hat{T}} v(T)\sigma(E',T)dT$$

$$= \int_0^{E_i} \sigma_d(E') \frac{dE'}{S(E')},$$

(2.132)

and

$$\int_{E_d}^{\hat{T}} v(T)\sigma(E',T)dT \equiv \sigma_d(E'),$$

(2.133)

where $E' = E'(x)$ is the ion energy as a function of the traveled path length $x$ as the ion travels down to zero energy. We can work a simple example using an approximation to the treatment given above. We are interested in the number of collisions made by an ion as it passes through a solid. We will take $I$ as the ion flux in units of ions/cm$^2$ s, and we can write the number of collisions per second in a volume element of unit cross-sectional area and thickness d$x$ which transfer energy in the range $(T, dT)$ to atoms of this element as:

$$NI\sigma(E,T)dx.$$

(2.134)

The number of collisions per unit volume per unit time which transfer energy in $(T, dT)$ at depth $x$ is $NI\sigma(E, T)$ [collisions/cm$^3$ s]. The number of displaced atoms for each collision that produces a PKA of energy $T$ is $v(T)$. Therefore, the production rate of displaced atoms at depth $x$ is as follows:

$$R_d(x) = NI \int_{E_d}^{\gamma E} \sigma(E,T)v(T)\,dT \quad [\text{displacements/cm}^3\text{s}].$$

(2.135)

(Note that we have not accounted for the fact that $I$ is a function of $x$ (or $E$) and that $I(x) \neq I_0$.) $E$ is a function of $x$ since the ion slows down by loss of energy to the electrons of the target. The functional form of $E(x)$ can be estimated using d$E$/d$x = kE^{1/2}$ as:

$$E(x) = \left[(E_i)^{1/2} - 1/2kx\right]^2,$$

(2.136)

where $E_i$ is the initial energy of the ion when it strikes the target. The number of displaced atoms/atom/s is $R_d(x)/N$, and the $\dfrac{\text{dpa}}{(\text{ions/cm}^2)}$ at a depth $x$ is $R_d(x)/NI$. We will assume that $\sigma(E, T)$ can be described by Rutherford scattering, and using the Lindhard treatment for $v(T)$ from the K–P model and assuming $\xi = 0.5$ gives:

$$\frac{R_d}{NI} = \int_{E_d}^{\gamma E_i} \frac{1}{2} \frac{\pi Z_1^2 Z_2^2 \varepsilon^4}{4} \left(\frac{M + M_i}{M}\right)^2 \frac{1}{E_i} \frac{4 M_i M}{(M + M_i)^2} \frac{1}{T^2} \frac{T}{2E_d} dT$$

$$= \frac{\pi Z_1^2 Z_2^2 \varepsilon^4}{4 E_i E_d} \left(\frac{M_i}{M}\right) \ln \frac{\gamma E_i}{E_d} \frac{dpa}{ion/cm^2}. \tag{2.137}$$

Applying this result to 0.5 MeV protons in iron gives $\sim 10^{-18}$ dpa/(ions/cm$^2$) at the surface. 20 MeV C$^+$ ions incident on nickel produce $\sim 3 \times 10^{-18}$ dpa/(ions/cm$^2$) at the surface, but 50 times this amount at the damage peak. These values can be compared to the damage rate from 0.5 MeV neutrons in iron:

$$\frac{R_d}{N\phi} = \left(\frac{\gamma E_i}{4 E_d}\right) \sigma_s$$

$$= 350 \times 3 \times 10^{-24} \tag{2.138}$$

$$= 1 \times 10^{-21} \frac{displacements}{n/cm^2}.$$

Comparing 0.5 MeV neutrons to 20 MeV C$^+$ ions shows that over their range C$^+$ ions produce 3000 times more displacements than do neutrons. Figure 2.25 compares the displacement rates as a function of penetration depth for ions of various mass and energy. As expected, for the same energy, ions of heavier mass deposit their energy over a shorter distance resulting in higher damage rates. Note that due
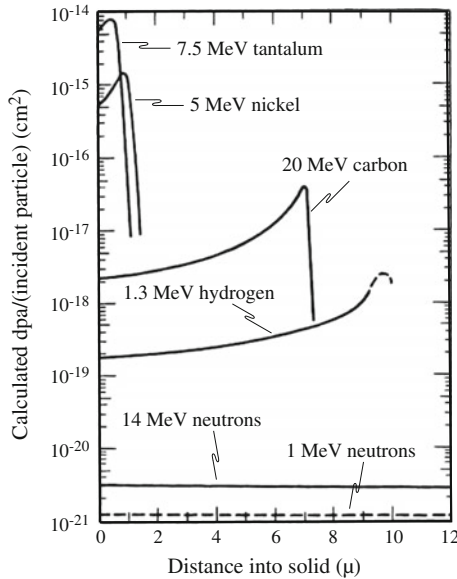


**Fig. 2.25** Displacement-damage effectiveness for various energetic particles in nickel (after [25])

to the large collision mean free path of a neutron as compared to an ion, the neutron damage energy is low and constant over distances of millimeters.

## Nomenclature

| | |
|---|---|
| $a$ | Lattice constant |
| $a_0$ | Bohr radius of the hydrogen atom |
| $A$ | Atomic mass |
| $A$ | Pre-exponential constant in Born–Mayer relation, Eq. (1.47) |
| $B$ | Spacing between barrier atoms in crystal lattice |
| $B$ | Constant in exponent in Born–Mayer relation, Eq. (1.47) |
| $c$ | Speed of light |
| $D$ | Nearest neighbor spacing between atoms |
| $E_c$ | Cutoff energy; critical energy for focusing |
| $E_{ch}$ | Critical energy for channeling |
| $E_{fc}$ | Critical focusing energy |
| $E_d$ | Displacement energy |
| $E_D$ | Damage energy |
| $E_i$ | Projectile energy |
| $E_r$ | Critical energy for replacement collisions; relative kinetic energy |
| $E_s$ | Sublimation energy |
| $E_\gamma$ | Gamma ray energy |
| $E_i$ | Incoming particle energy |
| $E'_m$ | Kinetic energy of incoming particle in CM system |
| $E''_m$ | Energy of neutron after (n, 2n) reaction |
| $E^*$ | Saddle point energy |
| $E_{eq}$ | Energy of atom in equilibrium lattice site |
| $f$ | Focusing parameter |
| $g$ | Relative speed $v_1 - v_2$ |
| $G$ | Damage function |
| $\bar{I}$ | Excitation–ionization level |
| $k$ | Force constant; constant in the electronic energy loss term, $kE^{1/2}$ |
| $m$ | Mass of incoming particle; 1⁄s in power law expression |
| $m_e$ | Mass of the electron |
| $M_1$ | Mass of projectile |
| $M_2$ | Mass of target |
| $N$ | Atom number density |
| $p$, $P_e$, $P_a$ | Probability, referring to electron and atom |
| $P_{ch}$ | Channeling probability |
| $P_d$ | Displacement probability |
| $P_f$ | Focusing probability |
| $Q$ | Excitation energy of nucleus |
| $r_{eq}$ | Equilibrium spacing between atoms |
| $r_{max}$ | Transverse amplitude of channeled atom |
| $R$ | Atomic radius |

| $R_{ch}$ | Radius of channel |
|---|---|
| $R_d$ | Displacement rate [#/cm$^3$ s] |
| $s$ | Exponent in the power law approximation |
| $S,\ S_e,\ S_n$ | Stopping power electronic, nuclear |
| $t_c$ | Collision time |
| $T$ | Energy transferred in collision |
| $\check{T}$ | Minimum energy transferred |
| $\hat{T}$ | Maximum energy transferred |
| $\bar{T}$ | Average energy transferred |
| $T_\ell$ | Energy transferred to target atom after (n, 2n) reaction |
| $U$ | Energy per atom in a crystal |
| $U_b$ | Binding energy lost by an atom when leaving a lattice site |
| $V(r)$ | Potential energy |
| $\upsilon_1$ | Velocity of projectile in laboratory system |
| $\upsilon_2$ | Velocity of target in laboratory system |
| $V_{CM}$ | Velocity of CM in laboratory system |
| $Y$ | Distance to atom barrier |
| $z$ | Impact parameter |
| $Z$ | Atomic number |
| $\beta$ | Compressibility |
| $\varepsilon$ | Secondary atom knock-on energy unit charge in Eq. (2.52) |
| $\varepsilon_{eq}$ | Energy of atom in a normal lattice site |
| $\varepsilon^*$ | Energy of atom at saddle point |
| $\in$ | Reduced PKA energy |
| $\phi,\ \Phi$ | Neutron flux, fluence |
| $\gamma$ | $4M_1M_2/(M_1 + M_2)^2$ |
| $\eta$ | Energy lost to electronic excitation in the NRT model |
| $\kappa$ | Displacement efficiency |
| $\mu$ | Reduced mass |
| $\upsilon$ | Specific volume of an atom |
| $\nu(T)$ | Displacement function |
| $\theta$ | Scattering angle in laboratory system |
| $\theta_c$ | Critical focusing angle |
| $\theta_{ch}$ | Critical channeling angle |
| $\sigma(E_i)$ | Total atomic collision cross section |
| $\sigma(E_i, T)$ | Differential energy transfer cross section |
| $\sigma_D$ | Displacement cross section |
| $\sigma_s$ | Scattering cross section |
| $\sigma_{sj}$ | Inelastic scattering cross section for the $j$th resonance |
| $\sigma_{(n,\ 2n)}$ | Cross section for (n, 2n) reactions |
| $\sigma_\gamma$ | Cross section for (n, $\gamma$) reactions |
| $\tau$ | Period for oscillation for a channeled atom |
| $\xi$ | Damage energy efficiency, Eq. (2.50) |

## Problems

2.1  (a)  Using the simple K–P model and assuming only elastic, isotropic scattering, calculate the number of displacements per atom (dpa) in nickel subjected to a fast neutron (2 MeV) fluence of $10^{22}$ n/cm$^2$

(b)  Using the relativistic expression for the electron–atom energy transfer, calculate the minimum electron energy required to displace an atom in (i) Al and (ii) W.

2.2  In a (n, 2n) reaction, a second neutron can only be emitted if the residual excitation of the nucleus after emission of the first neutron exceeds the binding energy of a neutron in the mass $M$ nuclide. The recoil energy after emission of the first neutron is taken to be the average value (cos $\phi$ = 0). Write an expression for the recoil energy following the second emission.

2.3  An $^{56}$Fe nucleus undergoes an (n, $\gamma$) reaction resulting in the release of a single 7 MeV gamma ray, on average. If a steel component is located in a reactor where the peak thermal flux is $1 \times 10^{14}$ n/cm$^2$ s and the thermal/fast flux ratio is one $\left(\text{where } E_{\text{ave}}^{\text{fast}} \geq 1 \, \text{MeV}\right)$, determine the relative displacement rates by fast neutrons, recoil nuclei, and gamma rays which undergo Compton scattering. Assume $\sigma_{(\text{n}, \, \gamma)} \sim 4b$, $\sigma_{\text{s}} \sim 3b$.

2.4  A slab of iron is exposed to a 20 MeV gamma source.

(a)  What is the most probable interaction between the gamma and the electrons in the Fe?

(b)  Assume the reaction you chose in part (a) occurs. Can this lead to the displacement of an Fe atom if the displacement energy is 40 eV?

2.5  A thermal neutron causes the following reaction

$$^{27}\text{Al} + \text{n} \rightarrow ^{28}\text{Al} + \gamma.$$
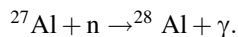
The gamma energy is 1.1 keV. The gamma will interact with lattice electrons. What is the most probable event? For this event, what is the maximum energy transferred? Does the resultant electron have enough energy to displace an aluminum atom (assume the displacement energy is 25 eV). Can the recoil Al atom displace another aluminum atom?

2.6  The (n, $\gamma$) reaction in $^{56}$Fe releases a prompt gamma ray of energy $E\gamma = 7$ MeV.

(a)  What is the recoil energy of the $^{57}$Fe product nucleus?

(b)  Determine the number of displaced atoms per $^{57}$Fe recoil assuming $E_{\text{d}} = 40$ eV.

(c)  If the thermal component of the neutron flux in a fast reactor is $10^{13}$ n/cm$^2$ s, what is the damage production rate due to the (n, $\gamma$) reaction in $^{56}$Fe?

(d)  If the fast flux is given by $\phi_f (E_n) = 10^{15}\delta (E_n - 0.5)$, where $E_n$ is in MeV, what is the damage production rate due to the fast flux in iron? Use the K–P displacement formula in (c) and (d). The scattering cross section for 0.5 MeV neutrons is 3 barns. Also, $\sigma_a^{56} \sim 2.5$ barns for part (c).

2.7  Assuming that atom–atom interactions can be treated as near head-on collisions, the appropriate potential function is then the Born–Mayer potential. Write an expression for the threshold energy for unassisted critical focusing along the [110] direction in fcc nickel in terms of the lattice constant, $a$.

2.8  For iron (equilibrium phase for 400°C), assuming a focusing collision occurs, how much does the closest approach (the allowed equivalent hard sphere radius calculated using a Born–Mayer potential) change between a [100] collision chain and a [110] collision chain?

2.9  (a)  Calculate the focusing energy of the $\langle 111 \rangle$ direction for gold under the condition of assisted focusing.
     (b)  Will focusing occur along the $\langle 111 \rangle$ direction in the absence of assisted focusing? Why?
     (c)  The experimental focusing energy of gold is 21,000 eV for the $\langle 111 \rangle$ direction. Compare your answer with this value.

2.10  (a)  Determine the critical focusing energy for the $\langle 111 \rangle$, $\langle 110 \rangle$, and $\langle 100 \rangle$ directions in fcc copper and iron.
      (b)  Plot $\theta_c$ as a function of $T < E_c$ for the $\langle 111 \rangle$ directions in Ni and Fe. Comment on similarities and differences.
      (c)  Do the same for the $\langle 110 \rangle$ direction of each.
      (d)  Repeat parts (a) and (b) using the inverse square potential, $V(r) = A/r^2$, where $A = 1.25$ eV nm$^2$.
      (e)  Over what energy range does focused replacement occur? How about focused energy packets only?

2.11  For the focusing process as described in Problem 2.10, give a physical explanation of why the critical angle for focusing, $\theta_c$, should depend on the projectile energy.

2.12  A 30 keV ion enters a channel in the solid lattice and loses energy only by electronic excitation. Using the Lindhard stopping power formula Eq. (1.191), determine the distance traveled by the ion before it is dechanneled. The minimum channeling energy is 300 eV. Use $k = 3.0NZ^{2/3}$ eV$^{1/2}$/nm, where N is the atomic density of the metal in nm$^{-3}$.

2.13  Show that when channeling is accounted for in the collision cascade, the average number of displaced atoms $v(T)$ is as follows:

$$v(T) = (T/2E_d)^{1-2p},$$

where $p$ is the probability that an atom with energy, $E$ being channeled is lost to the cascade. Assume that $p \neq f(E)$, $T \gg E_d$, and $p \ll 1$.

Assuming that all energy is lost by elastic collisions for 100 keV protons in nickel determine:

     (a)  The energy loss per unit length in the solid, $dE/dx$
     (b)  The range in the solid.

2.14   A crystal of copper is bombarded with monoenergetic (2 MeV) neutrons.

     (a)  Calculate the mean atomic displacement rate (displacements/cm$^3$s) using the simple Kinchin–Pease model and the following data:

        Lattice parameter, Cu = 0 361 nm
        Atomic weight of Cu = 63.54 amu
        Displacement energy for Cu = 40 eV
        $\phi = 10^{13}$ n/cm$^2$s (2 MeV)
        $\sigma_s = 0.5 \times 10^{-24}$ cm$^2$ (2 MeV)

     (b)  Repeat part (a) but instead of 2 MeV neutrons, use a monoenergetic thermal neutron beam with the same value of flux, $\sigma_{th} = 3.78 \times 10^{-24}$ cm$^2$ and the recoil energy $\sim 382$ eV.
     (c)  What would be the effect on your answer to part (a) by including Lindhard's damage energy function $\xi(T)$?
     (d)  How would your answer in part (a) be affected by assuming that the channeling probability is 1, 5, 10 %?

2.15   For the 2 MeV neutron bombardment problem described in Problem 2.14, how would you go about calculating the threshold energy for unassisted critical focusing along the [110] direction?

2.16   Assume that the copper target in Problem 2.14 was bombarded by a beam of 2 MeV He ions instead of a beam of 2 MeV neutrons. Calculate the displacement rate at the surface of the sample and compare to your result for Problem 2.14.

2.17   The same copper sample as in Problem 2.14 is bombarded with 500 keV Cu$^+$ ions at a flux of $10^{15}$ cm$^{-2}$ s$^{-1}$. Calculate:

     (a)  The displacement rate at the surface
     (b)  The location of the damage peak.

# References

1. Kinchin GH, Pease RS (1955) Rep Prog Phys 18:1
2. Seitz F (1949) Disc Faraday Soc 5:271
3. Bacon DJ, Deng HF, Gao F (1993) J Nucl Mater 205:84
4. King WE, Merkle KL, Meshii M (1983) J Nucl Mater 117:12–25
5. Olander DR (1976) Fundamental aspects of nuclear reactor fuel elements. US DOE, Washington, DC
6. ASTM E521 (1996) Standard practice for neutron radiation damage simulation by charged-particle irradiation. Annual Book of ASTM Standards, vol 12.02. American Society for Testing and Materials, Philadelphia

7. Robinson MT (1969) Defects and radiation damage in metals. Cambridge University Press, Cambridge
8. Snyder WS, Neufeld J (1955) Phys Rev 97(6):1636
9. Sanders JB (1967) Dissertation, University of Leiden
10. Kohler W, Schilling W (1965) Nukleonik 7:389
11. Sigmund P (1969) Appl Phys Lett 14(3):114
12. Lindhard J, Nielsen V, Scharff M (1968) Kgl Dan Vidnsk Selsk Mat Fyf Medd 36(10)
13. Sigmund P (1969) Rad Eff 1:15–18
14. Erginsoy C, Vineyard GH, Englert A (1964) Phys Rev 133A:595
15. Lindhard J, Nielsen V, Scharff M, Thomsen PV (1963) Dan Vidnsk Selsk Mat Fyf Medd 33:1
16. Robinson MT (1972) The dependence of radiation effects on the primary recoil energy. In: Corbett JW, Ianiello LC (eds) Proceedings of radiation-induced in metals, CONF-710601, USAEC Technical Information Center, Oak Ridge, TN, 1972, p 397
17. Norgett MJ, Robinson MT, Torrens IM (1975) Nucl Eng Des 33:50–54
18. Chadderton LT (1965) Radiation damage in crystals. Wiley, New York
19. Brandt W (1968) Sci Am 218:90
20. Datz S, Noggle TS, Moak CT (1965) Nucl Instr Meth 38:221
21. Doran DG (1971) Displacement cross sections for stainless steel and tantalum based on a lindhard model, USAEC Report, HEDL-TME-71-42. WADCO Corporation, Hanford Engineering Development Laboratory, Hanford
22. Robinson MT (1996) J Nucl Mater 216:1–28
23. Simmons RL, McElroy WN, Blackburn LD (1972) Nucl Technol 16:14
24. McElroy WN, Dahl RE, Gilbert ER (1970) Nucl Eng Des 14:319
25. Kulcinski GL, Brimhall JL, Kissinger HE (1972) Production of voids in pure metals by high-energy heavy-ion bombardment. In: Corbett JW, Ianiello LC (eds) Proceedings of radiation-induced voids in metals, CONF-710601, USAEC Technical Information Center, Oak Ridge, p 453